arXiv:1701.06568v1 [astro-ph.SR] 23 Jan 2017

ROYAL SOCIETY OPEN SCIENCE

rsos.royalsocietypublishing.org

Research

Article submitted to journal

Subject Areas:
astrophysics, extrasolar planets, stars

Keywords:
variable stars, protoplanetary disks, debris disks, circumstellar matter

Author for correspondence:
Grant M. Kennedy
e-mail: gkennedy@ast.cam.ac.uk

The transiting dust clumps in the evolved disk of the Sun-like UXor RZ Psc

Grant M. Kennedy[1], Matthew A. Kenworthy[2], Joshua Pepper[3], Joseph E. Rodriguez[4,5], Robert J. Siverd[6], Keivan G. Stassun[5,7], & Mark C. Wyatt[1]

[1] Institute of Astronomy, University of Cambridge, Madingley Road, Cambridge CB3 0HA, UK
[2] Leiden Observatory, Leiden University, PO Box 9513, NL-2300 RA Leiden, the Netherlands
[3] Department of Physics, Lehigh University, 16 Memorial Drive East, Bethlehem, PA 18015, USA
[4] Harvard-Smithsonian Center for Astrophysics, 60 Garden Street, MS-78, Cambridge, MA 02138, USA
[5] Department of Physics and Astronomy, Vanderbilt University, 6301 Stevenson Center, Nashville, TN 37235, USA
[6] Las Cumbres Observatory Global Telescope Network, 6740 Cortona Dr., Suite 102, Santa Barbara, CA 93117, USA
[7] Department of Physics, Fisk University, 1000 17th Avenue North, Nashville, TN 37208, USA

RZ Psc is a young Sun-like star, long associated with the UXor class of variable stars, which is partially or wholly dimmed by dust clumps several times each year. The system has a bright and variable infrared excess, which has been interpreted as evidence that the dimming events are the passage of asteroidal fragments in front of the host star. Here, we present a decade of optical photometry of RZ Psc and take a critical look at the asteroid belt interpretation. We show that the distribution of light curve gradients is non-uniform for deep events, which we interpret as possible evidence for an asteroidal fragment-like clump structure. However, the clumps are very likely seen above a high optical depth mid-plane, so the disk's bulk clumpiness is not revealed. While circumstantial evidence suggests an asteroid belt is more plausible than a gas-rich transition disk, the evolutionary status remains uncertain. We suggest that the rarity of Sun-like stars showing disk-related variability may arise because i) any accretion streams are transparent, and/or ii) turbulence above the inner rim is normally shadowed by a flared outer disk.

© 2014 The Authors. Published by the Royal Society under the terms of the Creative Commons Attribution License http://creativecommons.org/licenses/by/4.0/, which permits unrestricted use, provided the original author and source are credited.

THE ROYAL SOCIETY PUBLISHING

1. Introduction

Disks of gas and dust surround essentially all young analogues of our Sun (e.g. [1]). The lifetime of the gas in these disks is very short compared to the stellar lifetime, and within a few million years has accreted onto the star, been lost to space in photoevaporative flows, and contributed to building planets. The evolution of the dust during this phase is uncertain, but the existence of gas giant planets makes it clear that planetary building blocks, and of course some planets, form on a similar or shorter timescale.

Beyond the first few million years a typical star hosts a planetary system, the components being the planets themselves and a residual disk of small bodies. These "planetesimals" – the asteroids and comets – make up the "debris disk", where the standard picture is that destructive collisions between them generate a size distribution of fragments that extends down to micron-sized dust (e.g. [2–4]).

The state of planetary systems as they emerge from the gas-rich phase is uncertain. Planets' locations are not finalised at this epoch, but may move by interacting with other stars, planets, and/or planetesimals in the system (e.g. [5–7]). Similarly, the state and origin of the debris disk is uncertain. At stellocentric distances near 1au, the region of interest in this article, it could be that dust observed at this time is related to the final stages of planet formation (e.g. [8,9]), originates in young analogues of our Asteroid belt [10], is a signature of comets scattered inwards from more distant regions (e.g. [11]), or is simply a remnant of the gas-rich disk that has yet to be dispersed [12]. In the absence of gas detections that argue for the latter scenario, discerning among these various scenarios, which are not mutually exclusive, is difficult.

A promising way to probe these inner regions is by observing temporal variability (e.g. [13]). Optical and IR stellar variation has been studied for decades (e.g. [14,15]), and has recently been reinvigorated by large scale efforts (e.g. [16,17]) and as a side-effect of large-scale surveys for transiting planets [18,19]. Of many different classes of variables, the ones of most interest and relevance here are the "UXors", named for the prototypical system UX Orionis [15]. These are usually Herbig Ae and late-type Herbig Be stars [20], and typically show several magnitudes of extinction that is generally attributed to variable obscuration by circumstellar dust [15,21,22].[1] Three related arguments that favour circumstellar dust as the cause are i) a maximum depth of dimming events of roughly 3 magnitudes, suggesting that a few percent of the visible flux is not directly from the star, but scattered off a disk that surrounds the star and remains visible even when the star itself is completely occulted, ii) "blueing", where the star is reddened for small ($\lesssim$1mag) levels of dimming but returns to the stellar colour (i.e. becomes "bluer") for the very deep ($\gtrsim$1mag) events where the star is mostly occulted – the reddening indicates dimming by circumstellar dust, and a stellar colour is typical of light scattered off circumstellar dust [28], and iii) increased polarisation fraction during dimming events, caused by a greater fraction of the flux being contributed by dust-scattered light (e.g. [29], which also shows that the surrounding dust does not reside in a spherical shell). UXors therefore reveal information on the degree of non-axisymmetry, the "clumpiness", of dust orbiting a star on spatial scales similar to the star itself. The observations can span multiple orbits to test for repeated dimming events (e.g. [30]), and by using different bandpasses and polarisation can estimate dust grain sizes (e.g. [28,31]).

In the majority of UXor-like cases (i.e. those related to obscuration by dust), including other classes such as "dippers" (e.g. [17,32]), the processes causing young stars to vary are attributed to gas-rich protoplanetary disks. For Herbig Ae/Be stars the obscuration is thought to be caused by hydrodynamic turbulence that lifts dust above the puffed up inner rim of a self-shadowed disk [33]. For the dippers, which are observed around low-mass stars, the obscuration is attributed to dust in accretion streams that link the inner disk and the stellar surface, and/or to variations in the height of the inner disk edge [30,32,34]. The common theme is therefore that the location of

[1]Not all stars occulted by dust are UXors. Two other classes are: those occulted by circumstellar material beyond $\gtrsim$10au, such as AA Tau and V409 Tau which show $\gtrsim$year-long dimming events [23,24], and systems such as ϵ Aur, J1407, EE Cep, and OGLE-LMC-ECL-11893 where the occultations are attributed to circumsecondary disks (e.g. [18,25–27]).

the occulting dust is as close to the star as physically possible, being set by sublimation (e.g. [35]). These systems tell us about the nature of turbulence and accretion in gas-dominated disks, but so far reveal little about how these disks transition to the debris phase and the subsequent evolution.

Here we focus on RZ Psc, a star that shows UXor-like variability (e.g. [36–38]). As a young K0V type star with no evidence for gas accretion and a strong infrared (IR) excess, this system appears unique among UXors and may provide new information on the structure of inner planetary systems during or following dispersal of the gas disk [39,40]. However, the IR excess indicates the over 5% of the starlight is intercepted by the disk, which is a level more akin to gas-rich protoplanetary and transition disks than debris disks. Specifically, we use a decade of ground-based optical photometry of RZ Psc (section 3) to draw conclusions on dust location (section 4), and discuss the possible disk structure and evolutionary state in section 5. We conclude in section 6.

2. A clumpy dust ring near 0.5 au?

There is significant evidence that the optical variations seen towards RZ Psc are caused by circumstellar dust: i) during dimming events the colour becomes redder [36,41] in a way consistent with that expected for dust [42,43], ii) the maximum depth is about 2.5mag and during these events the colour returns to near stellar values, suggesting that the remaining emission is from light scattered off the circumstellar dust (i.e. the star is fully occulted [28,42], and iii) the polarisation fraction increases during the transits, as expected if an increasing fraction of the light is scattered off a disk of circumstellar dust [28,38,44].

What separates RZ Psc from other UXors (and dippers) is i) the spectral type is K0V rather than Herbig Ae/Be for UXors and late K to M-type for dippers, ii) the occulting dust lies well beyond the sublimation radius, and iii) the star is not associated with a star-forming region so is inferred to be a few tens of millions of years old. The dust distance has been inferred from the speed of ingress of dimming events, which was previously estimated as about 0.6au (for circular orbits [40]). Corroborating evidence comes from the $\sim$500K temperature of the dust seen in the mid-IR, which places it near 0.4-0.7au (depending on optical depth) and therefore at a location consistent with the occulting dust [40]. The distance to RZ Psc is unknown, but as an apparently isolated star that shows Li absorption the age has been estimated as a few tens of Myr, and therefore beyond the age at which a gas-rich disk would normally exist [39,45]. Further distinguishing features are that the duration of the dimming events is consistently short compared to other UXors, a few days rather than days to a few weeks, and that no near-IR (i.e. K-band) excess or accretion signatures are seen [45], so interpretations related to accretion of disk material onto the star (e.g. [21,30,34]) are unlikely.

Thus, the potentially compelling and unique aspect for RZ Psc is that we are observing dimming events from dust in a main-sequence planetary system that resides at about 0.5au. This dust is also seen in thermal emission, so deriving joint constraints on the dust properties and structure may be possible. As argued by de Wit et al. [40] a picture is emerging in which RZ Psc is surrounded by a massive young version of our own asteroid belt, in which planetesimals are continually being destroyed. These collisions generate the large collective surface area of small dust that emits strongly in the mid-IR, and the system geometry means that this dust also sometimes passes in front of the star.

While this asteroid belt picture is intriguing, and makes RZ Psc a system that could be of great interest and worthy of detailed study, it is not the only possibility. Well over 1% of the starlight is reprocessed by the circumstellar disk, which is more typical of the primordial gas-rich disks seen around nearly all young stars. The discovery of systems like HD 21997, that appear to be a few tens of Myr old and host gas-rich disks [46], shows that stellar age is not a perfect indicator of disk status. Thus, a considerable part of our analysis focuses on the question of the status of the disk around RZ Psc.

Given the proposed interpretation related to individual planetesimal disruptions, rather than hydrodynamics, it is perhaps surprising that to date the dimming events are not seen to be

periodic [40,47]. The only cyclical variation seen in light curves for RZ Psc is a 12.4 year variation with an amplitude of 0.5 mag, which is attributed to either a magnetic cycle, or precession of an otherwise unseen outer disk due to perturbations from an unseen companion [40].

3. Time series photometry

(a) Optical

To study the temporal variability of RZ Psc we use two seasons of public data from the Wide-Angle Search for Planets (WASP [48,49]), and nine seasons of data from the Kilodegree Extremely Little Telescope North (KELT-North [50]). We also collected, but ultimately did not use, photometric observations of RZ Psc from a wide variety of other sources ([15,36,41,44,51–53], the Catalina Sky Survey, the American Association of Variable Star Observers, the All-Sky Automated Survey). Aside from the Harvard plate photometry published by Gürtler et al. [37] we have not sought unpublished photometry so the light curve remains incomplete.[2]

Here we focus on the WASP and KELT-North data, as it has not been previously analysed and has considerably higher cadence (many measurements per night) and temporal coverage (nightly, weather permitting) than other data sets. The WASP data from 2004 and 2006 are public and were obtained from an online archive[3]. These data were processed in a manner similar to that described by [54], where common-mode variations were removed using 50 quiet nearby stars. The WASP bandpass is broad, with roughly uniform transmission from 400-700nm [48]. The KELT-North data, 2006-2014, were used in raw form, the only specific treatment being a 4% relative correction being made to ensure observations taken in the "east" and "west" telescope orientations have the same calibration. The bandpass is redder than for WASP, with most transmission between 500nm and 800nm [50]. For a full description of the KELT-North data reduction, see [55].

We normalised each year's data from each instrument separately by converting magnitudes to flux density and dividing out the sigma-clipped median so the light curve has an out-of-occultation baseline of 1. In doing so we are assuming that variations due to the slightly different filter bandpasses are unimportant. Each row in Figure 1 shows a season's data, starting on May 1 each year (JD also indicated). Most year's data therefore extend into the next year, so the "2006 data" refers to data from the 2006/2007 observing season.

(i) Qualitative light curve overview

It is clear from Figure 1 that RZ Psc undergoes the very deep dimming events that are typical of UXors. These are seen a few times each observing season and vary in complexity, with a few extended events (e.g. 2006) and a greater number of "neater" single events (e.g. 2010). In some years there is also significant variability at shallower depths. Of particular note is the pair of deep events in 2006; these appear to be about 70 days apart, and given the suggestion that the putative asteroid belt analogue resides near 0.5au a natural inference is that these two events are related. If true, this repetition corresponds to a semi-major axis of about 0.3au, which given uncertainties in the true disk spectrum could be consistent with the location of the asteroid belt. In 2004 there are about 100 days of near-consecutive nights of data and no deep events, so either the true period is longer than 100 days, or dust clumps can be created (and perhaps destroyed) on timescales of a year or so.

In Figure 2 we have selected most of the events from each year and shown them at a greater temporal resolution. The scale in each panel is the same, so wider boxes simply cover longer events. Most events appear to last at least a few days, suggesting that only having nightly coverage does not seriously hinder our ability to detect most events. However, the events are sufficiently short and irregular that the true shape of events remains uncertain. While it is likely that interpolation of the photometry for the fourth event in 2011 (that is, the fourth box from

[2]All normalised photometry is available at https://github.com/drgmk/rzpsc
[3]http://wasp.cerit-sc.cz

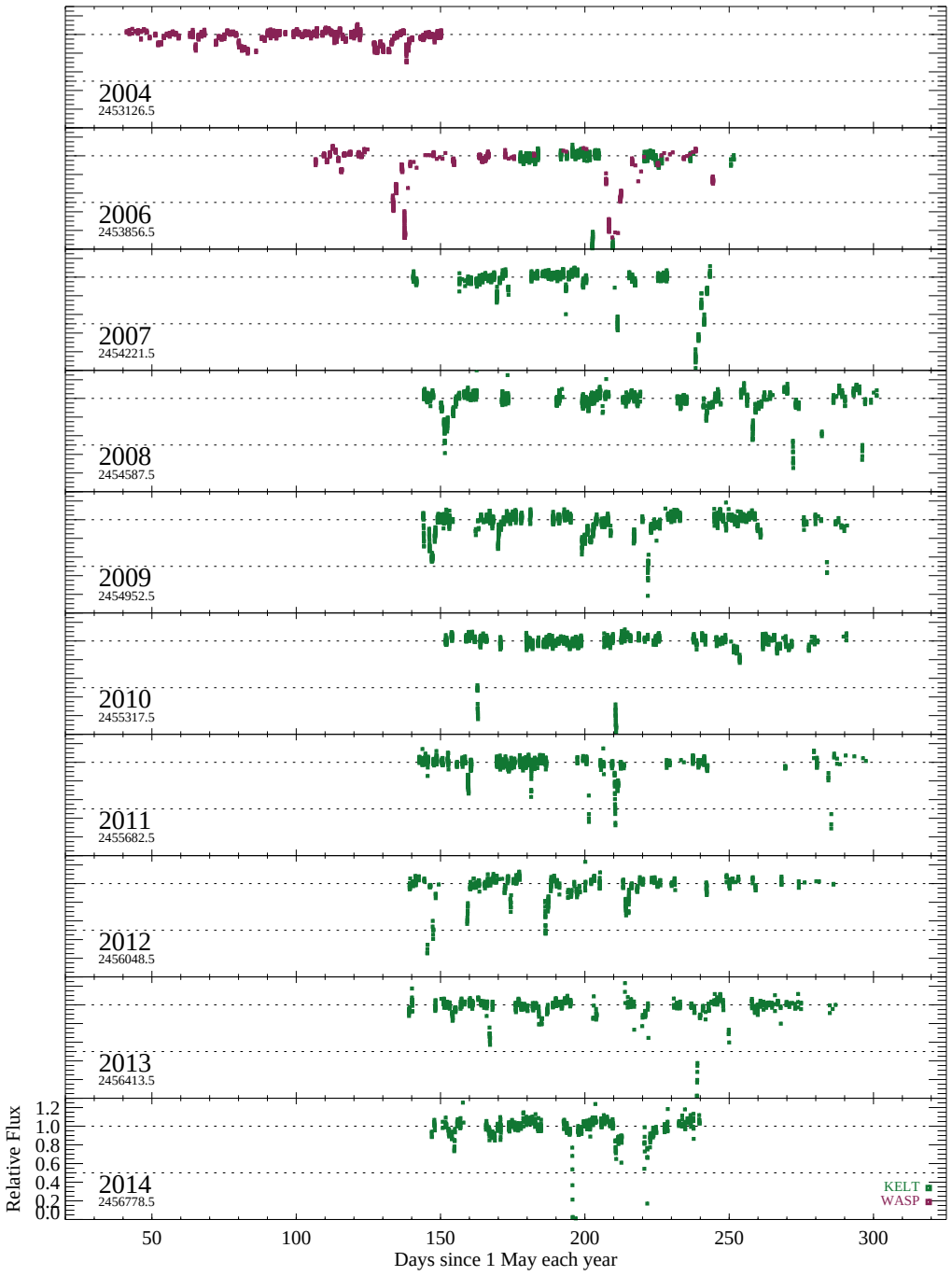

Figure 1. WASP and KELT-North data. Photometry is shown in dimensionless form, relative to a quiescent level of 1, and was converted from observed magnitudes as described in the text.

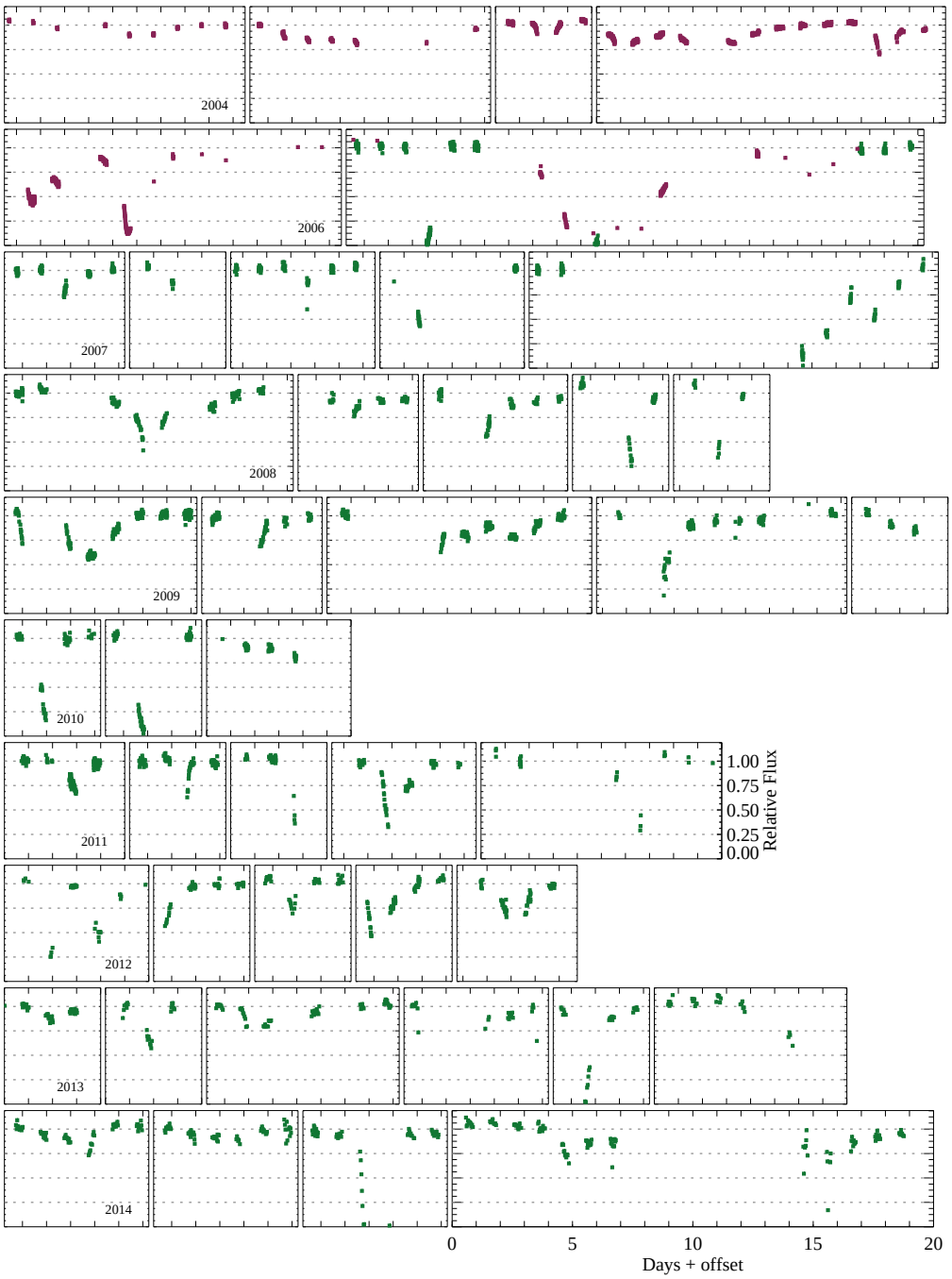

Figure 2. WASP and KELT-North data, focussing on dimming events. The vertical and horizontal scales in each sub-panel are the same.

the left in the row corresponding to 2011 in Figure 2) would resemble the true light curve, this assumption seems very unlikely to yield the true evolution of more complex events like those in 2006.

Nevertheless, Figure 2 shows an unprecedented view of dimming events seen towards RZ Psc, and that key information on the ingress and egress of dimming events is present. The dimming rate is such that it can be resolved temporally, and hence the velocity and radial location of the dust clumps estimated. While such estimates have been made in the past based on one or two individual events [36], these data make them possible for an ensemble of tens of events.

A fairly basic question is whether the light curve could result from objects that all have the same properties, or whether a range is required. Given the existence of both long shallow events and short deep events, at a minimum the clumps must vary in size and/or velocity across the face of the star, but probably also have different optical depths. The star can be completely occulted, so the clumps can be optically thick and star-sized, but it has already been shown that the events are not grey in colour, so the clumps must have a density gradient rather than sharp edges. Where sufficient data exist, it is clear that not all events have the same relative shape, so the shape of the clumps varies. Thus, the broad picture is of roughly star-sized clumps, whose shape and orbital elements vary. The fact that the dimming events can be shown in a series of panels with the same scale in Figure 2 suggests that the range over which these properties vary is of order factors of a few, not many orders of magnitude.

(b) Infrared

While the optical photometry reveals information about how RZ Psc is itself dimmed, IR photometry beyond a few microns is dominated by emission from the circumstellar disk. Thus, IR variation reveals information about how the emitting surface area, temperature, and perhaps composition, of the dust change with time. Such variation is indeed apparent, both from comparison of an AKARI 18μm non-detection at a lower level than the WISE 22μm detection, and from several individual WISE measurements taken at 6-month intervals.

Motivated by this variation, we obtained VLT/VISIR observations of RZ Psc; an N-band (10μm) spectrum on 2016 August 16 and Q-band (18μm) photometry on 2016 July 27 (programme 097.C-0217). These data, and the related calibration observations, were reduced using the standard ESO `esorex` pipeline. The wall-clock integration time for the spectrum was 50 minutes at an airmass of 1.66, and was calibrated using an observation of HD 189831 taken immediately afterwards at an airmass of 1.63. The spectra in individual chop/nod cycles are consistent so the shape of the spectrum is reliable. The absolute calibration is uncertain at $\sim$10% levels [56], which is sufficiently precise for our purposes here. The spectrum was trimmed to mask highly uncertain regions shortward of 8μm, and longward of 13 μm, and near the telluric absorption at 9.5μm. The Q-band photometry took 45 minutes at an airmass of 1.65-1.7, and was calibrated against an observation of HD 2436 taken immediately afterwards at an airmass of 1.5. Photometry of RZ Psc and HD 2436 was done using a 0.9″ radius aperture and a sky annulus from 1-2″. In addition to the conversion from adu/s to Jansky using HD 2436, we applied an additional upward correction to account for the slightly lower airmass for the calibrator ($\exp(0.3[1.675 - 1.5] \approx 1.05$, where an extinction of 0.3 per unit airmass was used, derived from archival calibration data using a method similar to that of Verhoeff et al. [57]). Uncertainties were estimated as the standard deviation of the flux density in 50 apertures around RZ Psc. The final calibrated flux is 86 ± 10 mJy.

The VISIR spectrum and photometry are shown in Figure 3, which also shows the other available near- to far-IR photometry. The absolute level of the spectrum agrees well with the IRAS, WISE (from the ALLWISE catalogue), and AKARI observations; that four observations spanning over 30 years are consistent suggests that while this part of the spectrum may vary, the shape and level shown is typical. The same cannot be said near 18μm, where the AKARI and VISIR (and perhaps WISE depending on the disk spectrum) flux densities are inconsistent. The flux near 10μm being relatively constant, and the 18μm flux changing could be indicative of shadowing of an outer disk by an inner disk; that is, evidence that the disk around RZ Psc has significant

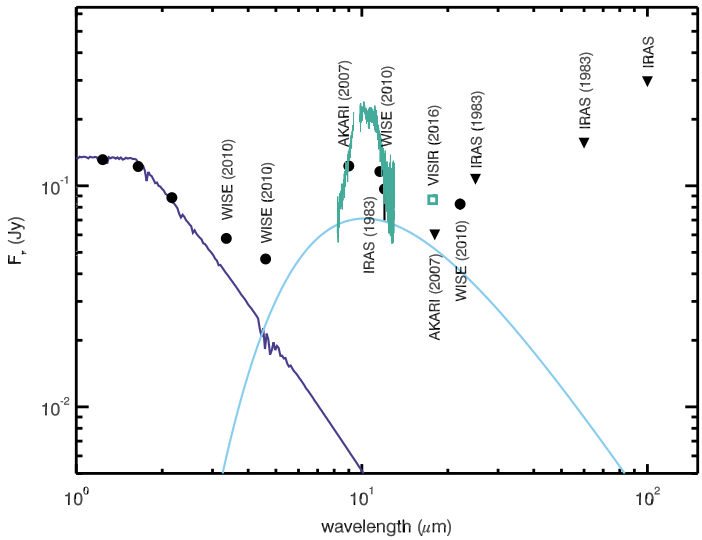

Figure 3. Flux density distribution of RZ Psc, including 2MASS, WISE, AKARI, VISIR, and IRAS data and their (approximate) year of observation. The dark blue line shows a stellar photosphere model at the approximate stellar temperature of 5350K, and the light blue line a 500K blackbody. The latter is not a fit, but an approximate continuum level that illustrates that the WISE 3.4 and 22μm photometry cannot both be accounted for with a single blackbody, if the silicate feature seen with VISIR was present in 2010.

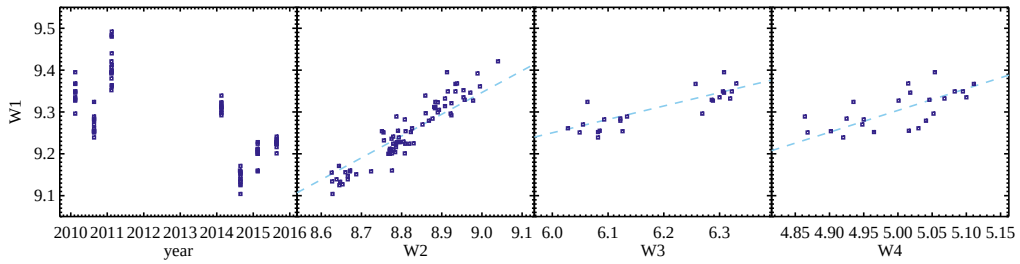

Figure 4. WISE epoch photometry at 3.4, 4.6, 12, and 22μm (W1, W2, W3, and W4, in magnitudes). The left panel shows the time variation in W1 over 5.5 years. Subsequent panels show how W1 correlates with W2, W3, and W4, which do not have observations at all W1 epochs. The dashed lines show the slope expected for constant disk flux variation with wavelength (the variation is smaller in W1/2 because the total flux is not dominated by the disk).

radial extent. This type of behaviour is seen as "seesaw" variability in IR spectra towards some transition disks (e.g. [58,59]).

The spectrum clearly shows solid-state emission (and the continuum level is not actually clear), which indicates i) that the dust is of order microns in size, and ii) that the dust includes silicates. The smooth rise and fall suggests that the silicates are largely amorphous; crystalline silicates have sharper features, notably a depression between two peaks at 10 and 11 μm, rather than the flat top seen here. Other systems thought to host bright asteroid belt analogues (rather than gas-rich disks), such as HD 69830, BD+20 307, and HD 113766A, tend to show crystalline features (e.g. [60–62]), which may argue against such a scenario for RZ Psc. However, such comparisons are largely speculative as there is also a high degree of variation among silicate features, for both gas-rich and gas-poor disks.

To further explore this variability, we use the WISE "epoch" photometry, for which the telescope scanning strategy results in clusters of measurements that are spaced 6 months apart. These data appear at approximately days 70 and 250 in the relevant years in Figure 1, but do not coincide with any optical dimming events. Photometry is not available in all four channels since launch in early 2010, due to exhaustion of the coolant after 7.7 months and a 2.5-year hiatus from mid 2011-2014 (see [63,64]). These data are shown in Figure 4, where the left panel shows the 3.4μm magnitude as a function of time, and that there is significant variation on 6-month timescales, and an even greater variation overall. Inspection of the individual clusters, which are on hour to day timescales, shows no significant variation with time. The dashed lines have the slope expected for disk brightness variation that is independent of wavelength; the slopes are not exactly 1 because the total flux is not dominated by the disk near 3-5μm, and hence the slopes are slightly flatter. Comparing the observed and expected correlations, we conclude that the data do not show significant evidence for changes in the spectral shape (i.e. changing temperature or composition). However, the ratios including 12 and 22μm observations are most sensitive to these changes, but only include the first two sets of observations where the brightness changes were relatively small.

Nevertheless, the amplitude of the change in 3.4μm brightness over 5 years is about 30%. Considering that the disk flux density is only 45% of the total flux at this wavelength, the disk brightness increased from 2010 to 2015 by about a factor of two. A similar variation can be inferred by comparing the 18μm upper limit from AKARI in 2007 and our VISIR measurement in 2016. Given these increases is it surprising that the N-band spectrum does not appear much higher than the IRAS, AKARI, and WISE photometry. A possible explanation would be that the increased emission originates in larger grains, which would result in greater continuum flux but similar levels in spectral features. However, without wider spectral and more frequent temporal coverage quantifying such effects is difficult. This level of IR variation is seen towards both protoplanetary (e.g. [58,65]) and debris disks (e.g. [13,66,67]), so these data provide little means to distinguish between scenarios.

4. Where are the occulting bodies?

The main part of our analysis concerns attempts to extract information from the optical light curve, taking advantage of the great number of dimming events seen over ten seasons. In this section we focus on the radial location of the bodies ("clumps") that pass in front of RZ Psc, first searching for periodicity associated with repeat events, and then using the light curve gradients to constrain the projected velocities. This analysis primarily focusses on what can be gleaned from the light curves, and the implications of these results for different clump origins are then explored in section 5.

(a) Search for periodic dimming events

We begin by estimating the lifetime of an occulting clump as a check on the plausibility that dimming events should repeat. The angular rate at which clumps are sheared out is $R d\Omega/dR = -3\Omega/2$. Accounting for shear in both forward (interior) and backward (exterior) directions the shear velocity across a clump of radius $R_{\rm cl}$ is then

$$v_{\rm sh} = 3R_{\rm cl}\Omega\,, \tag{4.1}$$

so the clump expansion rate due to shear in units of clump radii is only three times the orbital frequency. That is, after one orbit a clump will be stretched by a factor of 6π, and the radial and vertical optical depth will be roughly 6π lower (though it might still be optically thick). Thus, clumps that are not bound by their own self-gravity are expected to have a short lifetime at optical depths that are large enough to cause detectable dimming events, but could cause repeated dimming events if they are initially optically thick.

The temporal coverage of the observations in an individual season is 100-150 days. Thus, if the occulting material resides in an asteroid belt closer than ∼0.5au, periodicity in the dimming events may be visible in a single season's data. Longer orbital periods may be visible across seasons, though the six-month gap between seasons makes unambiguously linking events harder. Non-detection of periodicity would imply that the data are not sufficient, or that strict periodicity does not exist. An intermediate possibility is that occultations happen with a range of periodicities, perhaps reflecting their origin in a radially broad region, and that discerning this scenario from randomly occurring occultations is not possible given the data.

In an attempt to find the expected periodicity we tried several approaches. These are similar in that they aim to quantify whether some feature in the light curve is repeated again at a later time, but differ in how well they reveal evidence for a periodic signal. We found no evidence for events that are related from one year to another, so focus on statistics derived from individual seasons' data (though these are sometimes combined).

(i) Autocorrelation

We first used autocorrelation to search for periodicity, rather than methods related to Fourier transforms (e.g. periodograms). The motivation being that an individual transit event may be followed by another some number of days later, and perhaps repeat a few times, but other similarly (but not exactly) separated events may happen years later or earlier with a phase that is totally different. We therefore used the discrete autocorrelation function (DACF) proposed by Edelson & Krolik [68], though do not include uncertainties on individual measurements. For a time series with measurements a_i at times t_i the DACF first computes the mean $\bar{a}$ from the light curve, here we used the sigma-clipped mean to remove the dimming events. Then for each pair of points a_i, a_j (with $i \neq j$) computes $U_{ij} = ((a_i - \bar{a})(a_j - \bar{a})/\sigma_a$, with each U_{ij} associated with a time lag $\Delta t_{ij} = t_j - t_i$. A series of time lags centered at times $t_{\rm lag}$ with width $\Delta t_{\rm lag}$ are then used as bins, and the average in each bin is the DACF. The DACF is not computed for lag bins with no data. The units of the DACF are standard deviations of the light curve σ_a (again calculated using sigma clipping).

The results are shown in Figure 5 for time lags (i.e. trial periods) of 10 to 155 days in half-day bins. Comparison of these with the light curves shows that the DACF recovers most, but not all, events. Conversely, not all DACF peaks are necessarily associated with real repeat events, as there may of course be multiple distinct clumps orbiting the star at any given time. Not all pairs of events show a strong DACF signal, as they can comprise only a few measurements and the mean for that $t_{\rm lag}$ dominated instead by a much larger number of measurements elsewhere in the light curve closer to the quiescent level (i.e. near $\bar{a}$). Our attempts to avoid this issue by using autocorrelation on interpolated data yielded mixed results; heavy filtering, such as setting all data above a given level to 1, was needed for results similar to the DACF shown in Figure 5.

While several strong peaks appear in the DACF of all data, most of these arise from 2006, as can be seen in the DACF when these data are excluded. Some peaks remain near 70 days, as well as at 120 and 145 days, and the latter two could be aliases of periods near 60-70 days, arising simply because an event was missed. That is, the irregular sampling means that absence of evidence of power at some period in the DACF is not evidence of absence.

The pair of events separated by 70 days in 2006 provides the strongest signal, and most other years also show events near this period (2007, 2009, 2011, 2012, 2013, 2014). To illustrate these numbers the topmost line in Figure 5 quantifies the number of years that show a peak, in 10 day bins. The peak of 7 years is at 65-75 days, which is suggestive but not conclusive because a K-S test shows that this distribution is consistent with being uniform in period.

(ii) Iterative event finding

In an attempt to avoid some of the difficulties arising from the DACF, we tried a similar approach that first identifies individual occultation events and then computes the time delays between them. The main aim was to identify and use all events in a way that avoids biases related to the

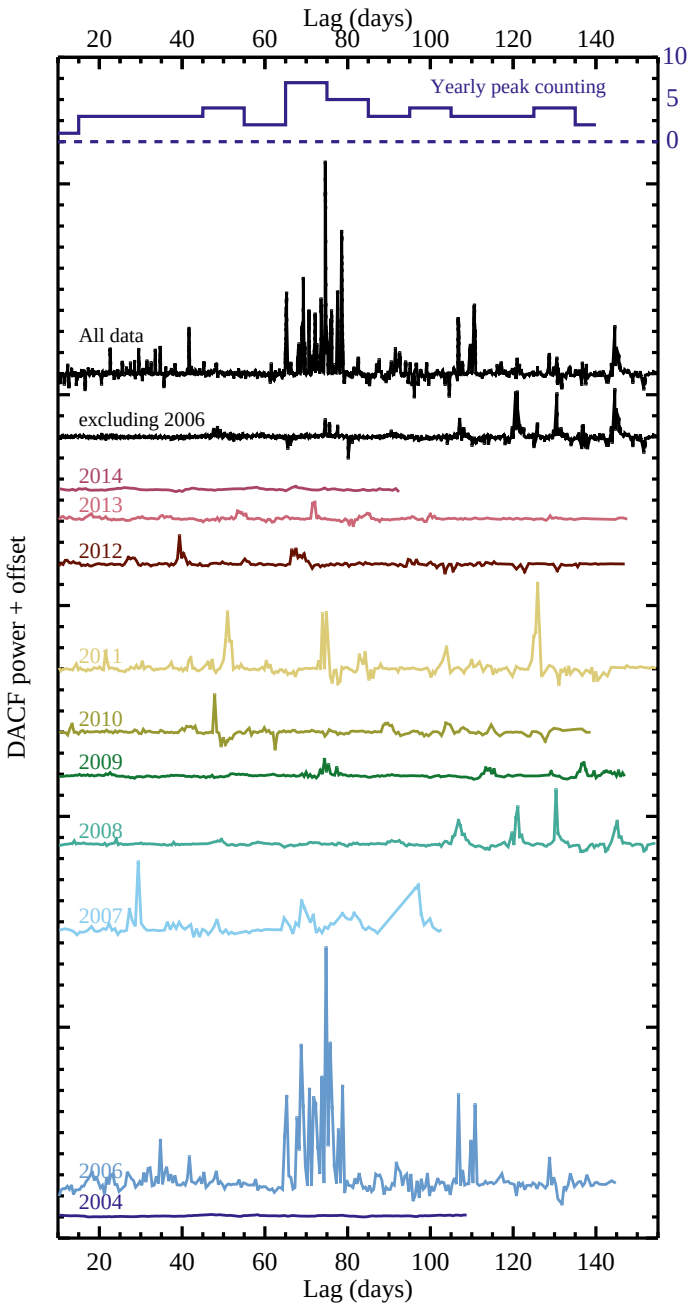

Figure 5. Discrete autocorrelation function for yearly WASP and KELT-North data, computed for lags between 10-155 days). The second and third lines from the top show all data, and 2006-excluded data. The topmost line shows the number of years that show a peak more than 3σ above the clipped DACF mean within each 5 day bin. The peak at 70 days is 7 years, the dashed line is zero, and the y-axis scale is shown to the right.

sampling of the data and the different relative depths of potentially repeated events. By repeating this prescription for synthetic data we are able to test different scenarios for how the occultations do or do not repeat.

For this approach, an event is initially identified as the lowest point that is 6σ below the mean, where the mean and standard deviation are again estimated by sigma-clipping. This lowest point is noted, as are all immediately adjacent points that are also below the threshold noted. The points so included constitute a single dimming event. The points belonging to this event are removed from the light curve and the process repeated until no significant events remain. The time of the event is the time of the lowest point, and the duration the time between the two end points that are consistent with the quiescent level. Thus, if an event is in a region of sparse sampling the duration can appear to be longer than it probably is, though we discard any events that occur at the beginning or end of an observing season to avoid unreasonably long events.

For a given set of event times and durations, the range of possible times between events is then calculated using the maximum allowed by the duration. This calculation is done for all combinations, yielding $N(N-1)/2$ inter-event time ranges. These ranges are then "stacked" into a histogram (i.e. counting +1 for time differences within a given bin) that shows a measure of the power present at a given time difference.

The solid lines in Figure 6 show this power in histogram form (the same in each panel), generated from 60 events that were identified in the light curve. The y-axis should be interpreted as the number of events that are consistent with that period on the x-axis. As before, there is evidence for a peak, now slightly shifted to near 65 days. In contrast to the DACF analysis, this power does not all arise from a single year. Most is contributed by 2004 and 2009, but exclusion of events from these years results in a similar (but noisier) histogram.

To test what could have been detected, and quantify the variation in power expected, we created synthetic light curves with the same temporal sampling as the WASP and KELT-North data. To do this we set the flux to 1, and randomly injected a number of dimming events with a flux of 0.1. These events are therefore relatively easy for the algorithm to detect, but suffer the same sampling issues. We tried individual randomly occurring events, and periodic events that repeat a fixed number of times. All events have durations randomly distributed between 1 and 4 days, similar to the observed events. For random events the remaining parameter in this model is simply the number of events – this is the total number over the 11 year period covered by the WASP and KELT-North data, including when measurements were not being taken. For repeating events the range of periods and the number of repeats are additional parameters. To estimate the level of variation in the power spectrum we repeated the process of injecting synthetic events 500 times, and in each bin estimate the mean and standard deviation of the power.

The results are shown in Figure 6, where the dashed lines show the mean and $\pm 1\sigma$ deviations from the simulations (and solid lines show the data). Each panel shows a different scenario, from top to bottom these are: 295 random events, 100 events with periods between 64 and 75 days and 3 repeats, and 100 events with a period of 64 days and 3 repeats. The purely random events are marginally disfavoured; while the data lie outside the dashed lines, these are only 1σ. Nevertheless, the middle and bottom panels show that the possible peak near 65 days could be caused by events with a range of periods, but that only a single period of 64 days is actually needed and yields a slightly stronger peak. The remaining excess periodicity near 10 days is not accounted for by any of the models, but could be an indication that on this timescale events are related (e.g. a clump that has separated into several). That the real signal nearly lies within the 1σ variation expected for randomly occurring events shows that the evidence for periodicity is weak, but that as found by the autocorrelation analysis, this weak evidence points towards 64 days as a possible period.

A side-effect of the simulations is an estimate of about 300 dimming events in total over the period between 11 June 2004 and 21 February 2015 (3851 days). On average an event therefore occurs about once every 13 days and there are 30 dimming events each year (and roughly 15 per

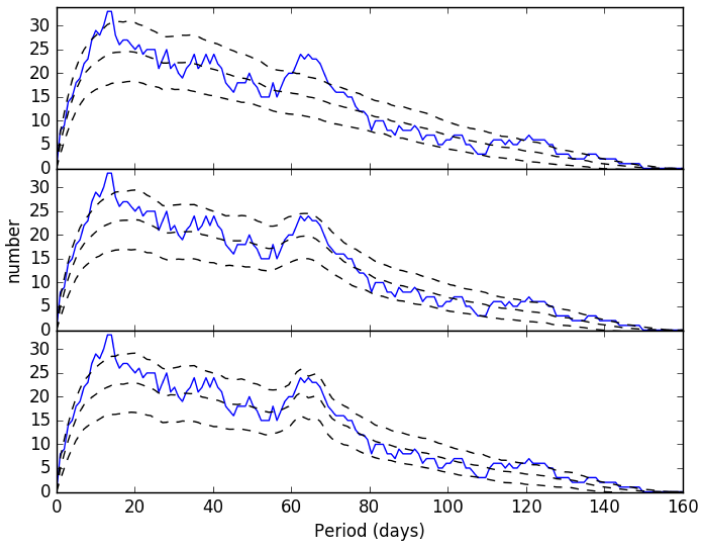

Figure 6. Power at a given period from the iterative event finding. The solid line shows the power from the data, and is the same in each panel. The dashed lines show the mean and $\pm 1\sigma$ power from simulated dimming events, which from top to bottom are: random, periodic between 64 and 75 days with 3 repeats, and periodic at 64 days with 10 repeats.

observing season). If events repeat three times, then a *new* dimming event would appear every 39 days on average, but we would also expect to see two other unrelated events during this time.

The total is five times larger than the 60 events detected by the iterative search. Most of these events were therefore either missed by the WASP and KELT-North observations, or not counted because they were mis-identified as single events. From Figure 1 a rough estimate is that 3 in 5 events would have been missed due to incomplete temporal coverage, meaning that about 1 in 5 simulated events were sufficiently close to other events that they were not separately identified. Not all events are deep, but as could be surmised from Figure 1, near continuous observation of RZ Psc would yield a rich light curve. If continuous coverage allowed closely occurring events to be separated, the number identified in a given time period would approximately double.

(iii) Summary of period search

We found a weak periodic signal near 60-70 days, but neither of the methods described above show compelling evidence that the dimming events seen towards RZ Psc are periodic and not random. While we presented results for single seasons' data, we saw no evidence for periodicity on longer periods. Aside from the 12 year variation, no periodicity has been seen in the past [40]. These searches used periodograms, which are sensitive to variations with fixed phase and poorly motivated, so we explored autocorrelation and a similar method. That we found a possible signal can be attributed to both a different method, and the significantly better temporal coverage of the WASP and KELT-North data.

A lack of strong evidence for periodicity is perhaps surprising, since material that occults the star once and is on an unperturbed orbit must pass in front of it again. Not all material need return at the same time however, and the prediction of the shearing estimate made at the outset, that the visible lifetime of clumps when they are optically thin is similar to the orbital period, appears to be borne out. Of course, shearing is not the only possible explanation, as pressure effects in a hydrodynamic turbulence scenario might also disperse a clump (as the sound crossing time for a star-sized clump near 1au is of order or shorter than an orbit). The latter scenario relies on a

significant gas reservoir, so the primary test to distinguish between different clump scenarios lies with the evolutionary status of the disk, which we explore in section 5(c).

(b) Gradient analysis

Given the possibility of a 60-70 day periodicity, the location of the occulting bodies could be relatively close to the star, with semi-major axes of about 0.3au. This distance is comparable to the 0.4au estimated for optically thin dust at 500K [40]. To further investigate the location we turn to a different aspect of the light curves that provides information on the velocity of the occulting bodies; the gradients. To convert gradients measured in the light curves to velocity and orbital distance, we first outline a simple model, and then use this model to interpret the data.

(i) "Curtain" model

This section considers a simple one-dimensional model (along x) of a cloud that dims a star. The main assumption is that the cloud is larger than the star, so for a cloud that passes in front of the star from left to right, the vertical (y) size of the cloud can be ignored. The large cloud extent is suggested primarily by the large depths of the dimming events, but also because no flat-bottomed (i.e. planet transit-like) events are seen. It seems likely that not all clumps are this large, and that a variety of sizes (and impact parameters) exist, but for our purposes this simplification is sufficient. Thus, the cloud is modelled as a semi-opaque screen or "curtain" that dims the star, as in previous analyses of related phenomena (e.g. KH-15D, J1407 [54,69,70]).

The star is dimmed by the passage of a cloud located at $x_{\rm cl}$ from the star center. The 1-D geometric optical depth structure of the cloud is given by some function centred at $x_{\rm cl}$ (e.g. a top hat or Gaussian) so is $\tau(x - x_{\rm cl})$. The star has a surface brightness $I(\sqrt{x^2+y^2})$, which could allow for limb-darkening. The observed flux from the star is then

$$F(x_{\rm cl}) = \int_{-R_\star}^{R_\star} (1 - \tau(x - x_{\rm cl}))dx \int_{-\sqrt{R_\star^2 - x^2}}^{\sqrt{R_\star^2 - x^2}} I(\sqrt{x^2+y^2})dy\,, \tag{4.2}$$

which first integrates vertically over the star at some x (i.e. independently of τ), and then along x, which includes the effect of the cloud. The light curve is therefore the convolution of the 1-D stellar brightness profile with the clump's optical "thin-ness" profile (i.e. $1 - \tau$). The flux profile (light curve) is a function of time, but the star and clump profiles are functions of x, and the conversion that links these is the cloud velocity.

The simplest case is a star of uniform surface brightness that is occulted by an optically thick screen that covers the star from $x = -1$ to u (i.e. the units of length are now $R_\star$). Then $I = 1$ and $\tau(x - x_{\rm cl})$ is a step function at u and the fraction of the total stellar flux ($F_\star = \pi$) seen is [69]

$$f = F/F_\star = (cos^{-1}[u] - u\sqrt{1-u^2})/\pi\,, \tag{4.3}$$

where f has the same units as our normalised light curve. If the curtain is not completely optically thick then the fraction is instead

$$f = F/F_\star + (1 - F/F_\star)(1 - \tau) \tag{4.4}$$

The gradient of the normalised light curve as the curtain is pulled across is df/du, and therefore the sky-projected (i.e. minimum) velocity of a clump is

$$\frac{du}{dt} = -\frac{\pi}{2\tau\sqrt{1-u^2}}\frac{df}{dt} \tag{4.5}$$

A cloud that is not completely optically thick has a shallower flux gradient because it reaches a shallower depth for the same velocity, and the factor $1/\tau$ accounts for this effect. Stated another way, for this curtain model the optical depth and cloud velocity are degenerate in producing some flux gradient. However, this degeneracy can be partially broken because some information on τ exists; τ must be greater than the depth of the dimming event (i.e. $1 - f_{\rm min}$, the minimum

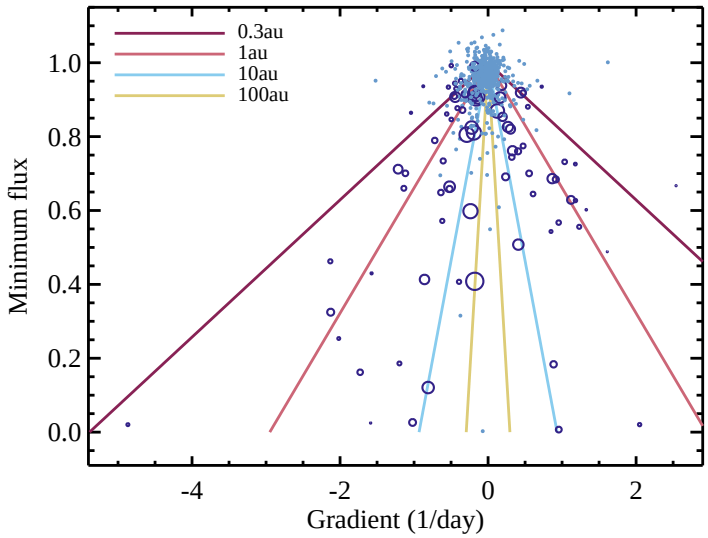

Figure 7. Gradient and minimum flux measured from individual nights' observations. Open circles have gradients significantly different from zero, and a symbol size proportional to the inverse of the gradient uncertainty. Dots are consistent with zero slope. The lines show the gradients implied by the velocities for circular orbits at 0.3, 1, 10, and 100au.

normalised flux). Objects somewhat smaller than the star are also accounted for; an optically thick clump that covers half the star produces approximately the same light curve as a $\tau = 0.5$ clump that covers the whole star.

These expressions can be further simplified by assuming that the maximum gradient occurs as the cloud "edge" passes the center of the stellar disk (i.e. $u = 0$). By adopting a radius for the star this velocity can be converted to physical units, and assuming a stellar mass and that the clump is on a circular orbit converted to a semi-major axis. If df/dt is in units of fractional stellar flux per day (i.e. the light curve is normalised and has time units of days) and du/dt in stellar radii per day (i.e. units of u are $R_\star$), then the numbers for these quantities can be used in the following equations:

$$v \approx 8050 \frac{R_\star}{R_\odot} \frac{du}{dt} \text{ m s}^{-1} \tag{4.6}$$

and

$$a_{\rm circ} = 14 \frac{M_\star}{M_\odot} \left(\frac{R_\odot}{R_\star} \frac{dt}{du} \right)^2 \text{ au} = 8.7 \frac{M_\star}{M_\odot} \left(\tau \frac{R_\odot}{R_\star} \frac{dt}{df} \right)^2 \text{ au} \tag{4.7}$$

While the assumption of $u = 0$ yields a simple conversion between the light curve gradient and the velocity and semi-major axis, it is of course possible to measure gradients that are not at $u = 0$. For example, the gradient when a dimming event reaches minimum is zero, which implies zero velocity and an infinite semi-major axis (e.g. the first minimum in 2006 in Figure 2). In addition, orbits may not be circular and thus the actual velocity is greater than the sky-projected velocity during a dimming event. Thus, the gradients and velocities must be taken as lower limits, and the semi-major axes as upper limits.

(ii) Curtain model application

Using the simple formalism described above, we can use gradients derived directly from the light curves to estimate the radial location of the occulting clumps. The gradients are estimated by least squares fitting straight lines to each night's observations, for which only nights with six or

more measurements are used. This procedure is possible because in nearly all cases an individual night's observations only cover ingress or egress, not both. These gradients are plotted against the minimum nightly flux $f_{\rm min}$ in Figure 7. We plot gradients whose uncertainty is less than $4\times$ their value as open circles, with symbol sizes proportional to the inverse of this uncertainty. All other gradients are plotted as small dots, as a check that the gradients for unocculted fluxes are near zero. The horizontal scatter of these gradients near $f_{\rm min}=1$ provides a further estimate of the uncertainty of individual gradients. The solid lines show the gradients expected for circular orbits at a range of semi-major axes.

An unusual feature in Figure 7 is that the gradients may be biased towards negative values at low $f_{\rm min}$. For the 15 negative, and 4 positive gradients below $f_{\rm min}=0.5$, and approximately equal numbers of positive and negative gradients above, Fisher's exact test yields a p-value of 0.02. Thus, there is evidence that the distributions of gradients above and below minimum fluxes of 0.5 are different, with negative gradients more commonly seen for deep dimming events. In the range $0.5<f_{\rm min}<0.8$ there are 15 and 25 negative and positive gradients, a reversal of the trend, but this difference only has a p-value of 0.1. Thus, there are about equal numbers of gradients measured with minimum fluxes below 0.8, but their distributions are different.

The bias to negative gradients below $f_{\rm min}=0.5$ suggests that ingress tends to be slower than egress; the egress is too quick to be caught. However, the equal numbers between $0.5<f_{\rm min}<0.8$ suggests that the rapid egress does not return the light curve to quiescence, just to a level above $f_{\rm min}=0.5$. Thus, the statistics suggest that a typical deep dimming event has an ingress at a rate of -1 to -2 day^{-1}, after which the flux rapidly rises to $f_{\rm min}\approx 0.5$, and then the remaining egress is at a rate similar to ingress.

Qualitatively, this inference is consistent with a scenario of a disrupted asteroid, whose structure is dictated by shear and radiation pressure. The fragment size distribution is such that at least half of the optical depth is contributed by grains large enough that their orbits relative to the original body are dominated by shear; forward shearing is more rapid than backward shearing, so the clump has a sharper rear edge than front edge, accounting for the different number of positive and negative gradients measured for $f_{\rm min}<0.5$. The fragments also comprise small grains whose dynamics are dominated by radiation pressure, which form a "tail" much like a comet's and account for the egress where $f_{\rm min}>0.5$. We leave the development of a quantitative study of this scenario for the future, noting that tests of such a model would require photometry at multiple wavelengths.

A look at specific dimming events shows that such a simple scenario will face challenges, as shown by the first set of events in 2006 (Figure 2); following the $f\approx 0.5$ dip there are two more nights of data that have higher average fluxes, but both nights actually have negative gradients. This evolution does not invalidate the above analysis, but shows that the temporal evolution is complex, and at any given time multiple clumps, which may or may not be related, could be occulting the star.

In Figure 8 we have converted the gradients into semi-major axes using equation (4.7). The dashed line shows the stellar radius, estimated to be approximately Solar based on an age of 25Myr [71] and an effective temperature of 5350K [45] using Siess et al. [72] isochrones. This Figure also includes solid lines of constant gradient, computed using equation (4.7) and $f_{\rm min}=1-\tau$.

The blue line shows the semi-major axis implied by the scatter in gradients near $f_{\rm min}=1$ in Figure 7. Above this line the gradients can be considered consistent with zero, and the inferred semi-major axes largely meaningless. A related point is that because the points near $f_{\rm min}=1$ have very small τ, the derived velocities and semi-major axes can be rather extreme and should be disregarded. An additional issue is highlighted by the two large circles near $f_{\rm min}=0.5$ and between $a_{\rm circ}=30$ to 100 au, which are the first two nights of 2006 observations shown in Figure 2. The first is at the time of minimum flux, and the other also appears to be at a turning point, so the assumption behind equation (4.7) that $u=0$ (i.e. the cloud edge is passing the stellar disk center) is clearly incorrect. These points should therefore be associated not with clumps at 30 to 100au, but with clumps that lie somewhere interior.

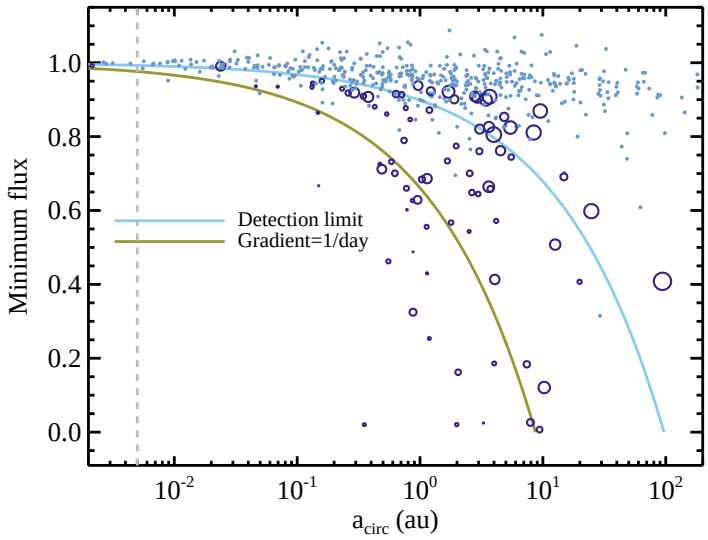

Figure 8. Semi-major axes estimated from the light curve gradients in Figure 7. Open circles have gradients significantly different from zero, and a symbol size proportional to the inverse of the gradient uncertainty. Dots are consistent with zero slope. The stellar radius (grey dashed line) has been estimated as Solar. Because gradients may have lower minimum fluxes they can move down along lines parallel to the solid lines. Points near or above the blue line are consistent with zero light curve gradient.

The green line shows the semi-major axis implied by a gradient of 1/day. As the lowest flux measured on a given night is not necessarily the minimum flux for that dimming event, the inferred semi-major axis could be greater; in this case points move downward parallel to this and similar lines. Figure 8 suggests that the clumps orbit with projected velocities that are consistent with circular orbits at or beyond about 1au. The conclusion from the IR excess, and possibly the periodicity analysis, is that they may lie closer, near 0.3-0.7au. Reconciling these differences requires that the clumps are on eccentric obits. For a semi-major axis of 0.3au the minimum clump eccentricity (i.e. all clumps transit at apocenter) is about 0.6. Such an orientation is of course highly unlikely, so either the semi-major axis is larger, or the true eccentricities need to be higher. Perhaps coincidentally, an eccentricity of 0.6 yields a pericenter velocity of 120km s^{-1}, similar to the velocity shifts in Sodium absorption lines seen towards RZ Psc, which are discussed further in section 5(b) (noting however that the pericenter velocity is tangential, and the absorption lines show projected radial velocity [73]).

(c) Summary of light curve analysis

The aim of this section was to estimate the location of the bodies that cause the dimming events towards RZ Psc. Using ten years of WASP and KELT-North data, we investigated both the periodicity of possible repeat events, and the light curve gradients. While we found evidence for a 60-70 day period, this signal is weak and not statistically significant. This period would place the clumps near 0.3au, similar to the distance inferred for the dust seen as an IR excess (though this location is also uncertain). The gradient analysis places loose constraints on the clump orbits (<10au), so is consistent with a scenario where the clumps have semi-major axes near 0.3au. Thus, based on the light curve analysis there is no reason to disfavour the model proposed by de Wit et al. [40], that the dimming events are associated with clumps being created by planetesimal collisions within an asteroid belt analogue.

The primary uncertainty lies with the disk evolutionary state. If a significant gas reservoir remains, a turbulent inner rim scenario similar to that proposed for UXors might produce a similar light curve. Both the lack of accretion, and a likely age beyond which gas-rich disks are typically seen, may argue against this scenario, though the disk may be in transition to the debris phase and retain some primordial gas. We revisit the disk status from the perspective of the flux distribution in section 5(c).

An additional result from the gradient analysis concerns the structure of individual clumps. The non-uniform gradient distribution is qualitatively consistent with post-collisional asteroidal fragments being dispersed by a combination of shearing and radiation pressure. Assuming small dust well-coupled to gas in a hydrodynamic turbulence scenario, a uniform gradient distribution seems more likely, so we interpret the gradients as providing circumstantial evidence for the planetesimal fragment scenario.

5. Disk structure and evolutionary state

Based on ten years of relatively high-cadence photometry, RZ Psc is regularly occulted by what are almost certainly star-sized clumps of dust. These clumps can be optically thick, and previous measurements of colour variations show that at least some of the dust must be small (e.g. [38]), which may be supported by the light curve gradient statistics. The previous interpretation of this system was that the clumps are the fragments arising from planetesimal collisions within an asteroid belt analogue that is also detected in the mid-IR. While the results from the previous section are consistent with this scenario, the evidence is at best circumstantial as they do not rule out the alternative of an UXor-like hydrodynamic inner rim scenario.

We now address several open questions, each taking a slightly wider view. Primary among these is whether the dimming events and the IR excess are caused by the same dust, as suggested by de Wit et al. [40]. Two further aspects are then the implications for the origin of the clumps and the evolutionary status of the disk in which they reside. We finish by considering the proposed scenarios for dippers and UXors, and why RZ Psc appears to be a rare object that lies between these classes.

(a) Does the occulting dust account for the IR excess?

One of the reasons that RZ Psc is worthy of detailed study is that circumstellar dust is inferred from both the dimming events and the IR excess. Different properties of the dust grains, and the larger structure in which they reside, are revealed by each method; the dimming events yield information on dust "clumpiness" on a star-sized scale, while the IR excess provides evidence for a disk that captures $\sim$7% of the starlight, and thus a measure of the total surface area of dust. The proposed interpretation is that the clumps orbit within an asteroid belt, and the dimming events therefore provide some information on the size distribution and collisional evolution within the belt [40]. This expectation relies on co-location of the clumps and the belt, for which circumstantial evidence is provided by the light curve gradients and perhaps the periodicity analysis (see also [39]).

The fraction of starlight intercepted by the dust is a variable common to both the dimming events and the IR excess. For the former we use the average extinction $\bar{E}$, which is simply taken from the normalised light curve, as 1 minus the average flux, yielding 0.05 (the light curve median is 0.995). This estimate assumes that all dimming events are independent, and the value would be smaller if not since the dust in some clumps may be being counted two or more times. The lack of strong evidence for periodicity suggests that multiple counting is not a serious issue however. Another issue is that the star could be reddened, and therefore that the normalised light curve has already had some constant level of extinction removed. Based on photospheric colours this unseen extinction is probably small, in the range of zero to a few percent [74].

If we assume that this average extinction applies over a uniform sphere around the star, and that the dust has a low albedo (i.e. the dimming events are dominated by dust absorption, not

scattering of light out of our line of sight), then the IR fractional luminosity is equal to the average extinction. That is, both are equal to the fraction of starlight intercepted by the dust.

To explore possible geometries we use a simple relation between fractional luminosity $L_{\rm disk}/L_\star$, (uniform) geometric optical depth τ, and the disk opening angle θ [12]

$$L_{\rm disk}/L_\star = \tau sin(\theta/2)\,, \tag{5.1}$$

which says that the fractional luminosity is the optical depth of the dust multiplied by the fraction of the sky covered as seen from the star. The dust belt must therefore have an opening angle of at least 8° to capture 7% of the starlight. However, for this minimal estimate the dust is optically thick, yet RZ Psc is not seen to be reddened. If we instead require $\tau \sim \bar{E}$ then as stated in the previous paragraph the dust distribution must instead be near isotropic. Given the ubiquity of disk-like structures around young stars, such a spherical distribution seems physically unlikely. In addition, the increased polarisation during deep dimming events argues against a spherical distribution.

Thus, the picture of RZ Psc as a star seen *through* a disk, where the clumps account for all of the dust and sample some representative part of an asteroid belt (e.g. the midplane), is untenable because that belt would cause much more reddening than is observed. These characteristics distinguish RZ Psc from heavily reddened objects, where the dimming events could be sampling a more representative section of the disk (e.g. [75]). This issue can be avoided by invoking a spherical distribution of material, but the problem then shifts to whether such a distribution is physically plausible.

A more likely alternative, which we favour, is that most of the dust does not lie on orbits that pass in front of the star, and the occultations are caused by a small fraction of objects that have higher vertical locations (or greater orbital inclinations) than average. In this case the component that causes most of the IR excess may or may not be clumpy, and could be radially optically thick (i.e. the opening angle could be as small as 8°). This picture unfortunately loses any strong connection between the occulting clumps and the IR excess, essentially adding a free parameter that is the fraction of material that is "kicked" or resides above the disk, but seems to be the simplest and most probable scenario. Dullemond et al. [33] used essentially the same argument for UXors, so our picture is therefore inevitably similar to dust occultation models proposed for UXors (e.g. [22,33,76]). As the disk is probably radially optically thick with a scale height similar to gas-rich protoplanetary disks, it could be that the scenario for RZ Psc is in fact the same as proposed for UXors. In this case, the IR excess would originate from the inner edge of a more extended disk, which is not detected at longer wavelengths for reasons discussed below.

We therefore conclude that while there is almost certainly some connection between the dimming events and the IR excess, it is at best indirect; we are not viewing RZ Psc through a representative part of an asteroid belt analogue. As with other UXors, a clear prediction is that the disk is not seen edge-on, but at an intermediate inclination.

(b) Origin of the occulting structures

One of the distinguishing characteristics for RZ Psc is the relatively short duration of the dimming events $t_{\rm dim}$, which are a few days compared to a few weeks for other UXors (e.g. [21,77]). If we assume near-circular orbits at speed $v_{\rm kep}$, $t_{\rm dim} = 2(R_{\rm cl} + R_\star)/v_{\rm kep}$, where the clump has radius $R_{\rm cl}$. Solving for the clump radius yields the relation (e.g. [32,78]):

$$R_{\rm cl} \approx 1.85 t_{\rm dim} \left(\frac{M_\star}{M_\odot}\frac{1{\rm au}}{a}\right)^{1/2} - R_\star\,, \tag{5.2}$$

where here $R_{\rm cl}$ and $R_\star$ are in units of $R_\odot$ and $t_{\rm dip}$ is in days. This equation says that dimming events of a given duration can in general be caused by larger clumps that orbit close to the star, or smaller clumps that orbit farther out.

Figure 9 shows the radius that clumps must have to cause dimming events of different durations as a function of semi-major axis. For clumps much larger than the star the stellar radius

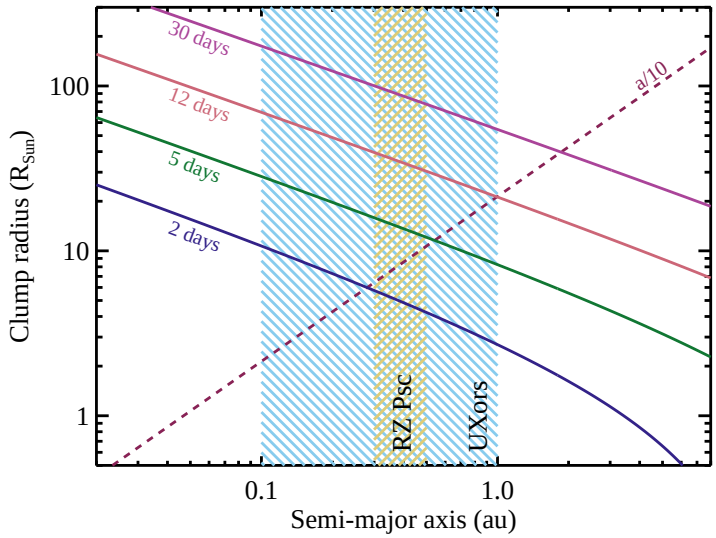

Figure 9. Clump properties assuming circular orbits for a range of dimming event durations (as labelled). The brown region marks the approximate location of the RZ Psc asteroid belt (or the inner edge of a more extended disk). The blue shaded region shows the range of Herbig Ae inner disk edge radii. The dashed line shows where a clump has an azimuthal extent similar to the scale height of a typical gas-rich disk.

is unimportant, and the stellar mass dependence is relatively weak, so this plot can be applied to RZ Psc and UXors. The radius is of course the sky-projected size of a clump along the orbit, so whether this scale also applies vertically and radially depends on the specific scenario. This plot assumes circular orbits, and that the star has Solar radius and mass. The approximate locations of the RZ Psc belt (or the inner edge of a more extended disk), and the range of inner edge radii for Herbig Ae stars [35], are shown by the hatched regions.

The dashed line shows where clumps extend a tenth of the semi-major axis - approximately the scale height for a gas-rich disk. If the variability of both UXors and RZ Psc originates from dust structures arising from hydrodynamic turbulence at the disk inner edge, and these structures are related to the disk scale height, then a wide range of dimming event times is expected. These times should correlate strongly with the inner edge location, and because this location is set by sublimation [35], should correlate with the luminosity of the star. We did not find evidence for such a correlation in time-variability studies of UXors (e.g. [79]), suggesting that the clump radii do not vary strongly with the inner edge location. In any case, we have already noted that RZ Psc has shorter dimming events than "typical" UXors, so while RZ Psc has dust at a radius that falls within the range of UXors, the occulting clumps are inferred to be several times smaller.

A further difference between RZ Psc and UXors is the origin of the dust location. For Herbig Ae/Be stars (and by extension, UXors) the dust inner radius is set by sublimation. However, the dust around RZ Psc is roughly 500K, so much cooler than the ∼1500K sublimation temperature. That is, if the origin of RZ Psc's variability is interpreted as similar to other UXors and originates in a gas-rich disk, it must host a transition disk rather than a "full" primordial disk. Therefore, while these comparisons show RZ Psc to be unusual compared to typical UXors, they do not argue strongly for or against a specific scenario.

A final aspect to discuss regarding the origin of the clumps, and their relation to the IR excess, is the transient absorption features. These are seen towards UXors, but also seen towards some main-sequence A stars (e.g. [80–82]), so are not exclusive to stars that host gas-rich disks. For A-type stars these features are generally interpreted as sun-grazing "exocomets", and the same may apply to UXors and RZ Psc. A potential issue with this interpretation is that the absorption lines

towards RZ Psc are so far blue-shifted, and may instead originate in an outflow [73]. However, blue-shifting could also occur if evaporation mostly occurs near periastron passage, which might be expected if the bodies originate in an asteroid belt and are thus more refractory than the exocomets seen towards other stars (i.e. an Asteroid in the Solar System would need to pass very close to the Sun to have a tail). Such a scenario is also consistent with the conclusion of section 4 that the occulting clumps could be on eccentric orbits with high velocities at periastron. Models of such low-periastron asteroids or comets invariably require a perturbing planet (e.g. [83,84]). Assuming the same 4:1 mean-motion resonance picture of Beust & Morbidelli [84] implies a planet about 2.5 times more distant than the source. That is, if the asteroid belt is at 0.3au, the planet is near 0.75au. It may be possible that this planet is inclined and causes the asteroid belt to precess, thus causing the 12.4 year modulation of the stellar flux seen by [40].

Overall, the origin of the clumps remains unclear, and raises many further questions. A distinguishing feature of RZ Psc's light curve is that most of the time the star is near the quiescent level; if the dimming events are related to variable structure at the inner rim of a gas-rich disk, then why are the events so rare? Is the geometry so finely tuned that only the most extreme fluctuations are visible? In the asteroid belt scenario the details are equally unclear; if the clumps are recently disrupted planetesimals, how do they appear above the bulk of the disk when collisions are most likely to occur at the mid plane? Are there two populations of objects, one that forms the main disk, and another that causes the dimming events? Could such a scenario be reconciled with the transient absorption features? Answers to these questions will require further study, and will almost certainly require new observations.

(c) Disk evolutionary state

Many young stars with gas-rich disks show broadly similar variability (UXors, AA Tau analogues, dippers). With sporadic and deep photometric minima, and transient absorption lines, RZ Psc is most similar to UXors and has often been associated with this class, albeit as an unusual member (e.g. [39]). Initial distinctions were made based on the late spectral type (K0V), the relatively short dimming events, and a lack of near IR excess and accretion signatures. The more recent findings that the stellar age is probably several tens of Myr, and that the IR excess is suggestive of an Asteroid belt analogue, further distinguish RZ Psc as a potentially remarkable object where the early gas-poor stages of main-sequence debris disk evolution can be studied. There remain similarities between RZ Psc and UXors. Primarily, we concluded that the clumps that cause the dimming events are most likely seen when they are well above the densest regions of a disk, consistent with the turbulent inner rim scenario proposed by Dullemond et al. [33].

To consider RZ Psc within the context of other young disk-hosting systems, Figure 10 shows the spectral energy distribution (SED) of RZ Psc, and several other systems that could be considered to be at a similar evolutionary stage (a similar plot appeared in [12]). GM Aur hosts a transition disk [85], the status of HD 166191's disk is ambiguous and may lie somewhere between the transition and debris phase [12,86], and HD 113766A is generally considered to host a bright warm debris disk (based on a 10-16Myr age and a lack of gas [87], but based on similarities with HD 166191 was also noted as potentially ambiguous [12]).

In contrast to UXors, there is no obvious reason for dust around RZ Psc to lie near 0.3 au, as the dust sublimation distance is much closer. For RZ Psc to host a gas-rich disk it would therefore probably need to be a transition object that has as-yet undetected far-IR emission from the outer disk. As illustrated by Figure 10 the limits set by IRAS are not particularly stringent, but in comparison to GM Aur the SED beyond 20μm is a factor of two lower, despite the mid-IR SED being a factor of two brighter. Transition disks have a wide variety of spectra however (e.g. [58,88], so the main conclusion from this comparison is that if an outer disk exists, it is not very bright. This far-IR deficit is a signature of self-shadowing, which is of course a key characteristic of UXors. If such a picture were true for RZ Psc, a prediction is that the outer disk may still be detectable at millimeter wavelengths (roughly mJy levels), whereas an extrapolation based on the asteroid belt scenario would not (roughly μJy). Specifically, self-shadowing can be caused by settling of dust

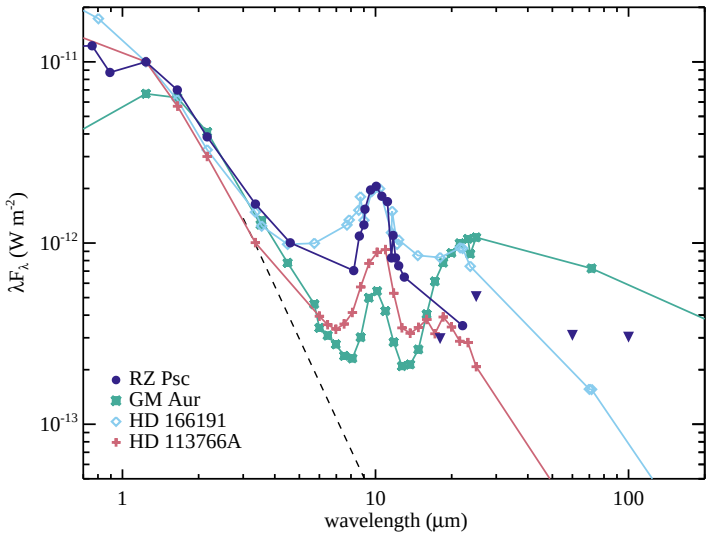

Figure 10. The SED of RZ Psc in comparison with other young disk-hosting stars. All SEDs are normalised to a common flux density at H band. The triangles are AKARI and IRAS upper limits for RZ Psc. Measurements we made at different times, so the apparent discrepancy between the WISE detection at 22μm and the AKARI upper limit at 18μm is an indicator of IR variability (see section 3(b)).

towards the disk mid-plane, which can occur with little loss of vertical optical depth [89]. Thus the far-IR flux can be much lower than for a typical disk, while the mm-wave flux is not.

In Figure 10, RZ Psc looks more similar to HD 166191 and HD 113766A, thus falling in the category of systems whose interpretation in terms of disk status is ambiguous (the high fractional luminosity would also mark RZ Psc as unusually extreme for a debris disk). With the aid of mid-IR interferometry, the disk around HD 113766A has been shown to comprise two components, one at 0.6 and another at 9au [90]. This is by no means evidence that RZ Psc has a similar structure, but merely reinforces the fact that the SED does not rule out such possibilities and that the dust need not be confined to a single belt near 0.3au, and need not be interpreted as an asteroid belt. Similarly, the disk around HD 166191 was modelled as an optically thick transition disk extending from 1-25au [12]. Thus, as was concluded above by considering self-shadowing, it could be that RZ Psc hosts a disk that extends from 0.3 to a few tens of au.

While the lack of a large near-IR excess for RZ Psc suggests that the disk is at least in the transition to a debris disk (i.e. has an inner hole), it does not preclude the possibility that gas resides in that hole and may still be accreting on to the star. No emission lines that would provide evidence of accretion have been seen [45,73], but as a further test we reconsidered the spectral energy distribution. Specifically, we included photometry from the Galaxy Evolution Explorer (GALEX [91]) to quantify the level of any ultraviolet (UV) excess, a complementary accretion indicator (e.g. [92]). This exercise is hindered somewhat by the possibility that optical photometry was obtained when RZ Psc was not near the quiescent level. To circumvent this issue we used just the Two Micron All-Sky Survey (2MASS [93]) and GALEX photometry, fitting a PHOENIX atmosphere model [94], finding a best-fit effective temperature of 5485K (assuming no reddening, or 5600K if some reddening is allowed to improve the fit slightly). These temperatures are consistent with that derived from a high-resolution spectrum; 5350 ± 150K [45]. Alternatively, fixing the temperature to the spectroscopic value yields a mild UV excess, less than a factor of two, that may be chromospheric. We therefore conclude that there is no evidence for accretion seen as a UV excess.

Finally, the mid-IR variability discussed in section 3(b) provides a measure of the changing emitting area of the disk around RZ Psc, and thus potentially information about the disk structure and status. Figure 4 shows that for the epochs where contemporaneous 3-22μm photometry exists there is no evidence of "seesaw" variability over 6 months, but that strong conclusions are limited by a lack of data. Over 5 years the 3-5μm disk flux varied by about a factor of two, with no major changes in the behaviour of the optical light curve. However, given that the bulk of the disk emission probably originates from material that is not occulting the star, direct links between the optical and IR behaviour is not necessarily expected. Indeed, towards young stars hosting gas-rich disks, both correlated and uncorrelated optical/IR variability is seen [17]. Similarly, the IR flux of bright warm debris disks has been seen to vary strongly while the optical brightness remains constant [95]. The main benefit of more intensive IR monitoring would be to search for mid-IR "see-saw" variability, because it would provide evidence that the disk around RZ Psc has a significant radial extent.

In summary, the status of the disk surrounding RZ Psc is unclear. Despite a reasonable near/mid-IR characterisation, at longer wavelengths the SED is not detected. Comparison with the infrared spectra of other disks suggests that the disk is at a minimum well evolved towards the debris phase, and may have reached it already. This possibility, and the rarity of objects like RZ Psc, opens the possibility that it is being observed at a special time with a specific geometry, so may yield better insights than most systems.

(d) The rarity of Sun-like dippers/UXors

We finish by briefly discussing RZ Psc in the context of the general classes of dippers and UXors, considering why neither of these classes includes many young Sun-like stars like RZ Psc. To aid this discussion, Figure 11 shows simplified cartoons of the proposed scenarios for dippers and UXors, and possible reasons for a lack of significant dust-related dimming events towards Sun-like stars (see [34] for similar figures for dippers).

From the perspective of dippers, which so far have spectral types later than K5, Bodman et al. [34] explain their tendency to be low-mass stars as a consequence of the relation between the magnetospheric truncation, corotation, and sublimation radii. The periodicity of dippers suggests that the occulting material is near the corotation radius, and is therefore near the base of any accretion columns. For low-mass stars the dust temperature at this distance is cool enough that the columns contain significant dust mass and hence the dipping phenomenon is seen (top panel of Figure 11. For earlier type stars the sublimation radius is outside the corotation radius, so any dust in the accretion columns has sublimated and no dipping is seen (grey accretion column in the middle panel of Figure 11).

An as-yet unexplored corollary of this scenario is that the outer disks in dipper systems must not be more flared than the height of the accretion columns (as seen from the star). This could be because disks around low mass stars are simply less flared in general (e.g. [96]), because disks in dipper systems tend to be more evolved than average [32], or because there is less relation between the outer disk geometry, the inner disk, and accretion columns than would be naively expected [97]. Of course, if disks around Sun-like stars are sufficiently flared that the inner regions are not visible, then whether the accretion streams are transparent or not is moot.

From the perspective of UXors, a possible explanation for their tendency to be late B and A-type stars is that the specifics of self-shadowing are different for Sun-like stars [33]. There is little reason to believe that self-shadowing does not happen for young Sun-like stars [89,98], so it seems either that self-shadowing is simply rarer, or that the nature is different in a way that affects whether the inner disk can occult the star (i.e. shadowing is by a larger portion of the inner disk regions rather than by a puffed-up inner rim, [89,99]).

Thus, it seems that the rarity of Sun-like stars among dipper and UXor populations may be understood as a result of the scenarios for both. Accretion columns are optically thin because the dust has sublimated, and any turbulence that rises above the inner disk may not be seen as it is hidden behind a flaring outer disk.

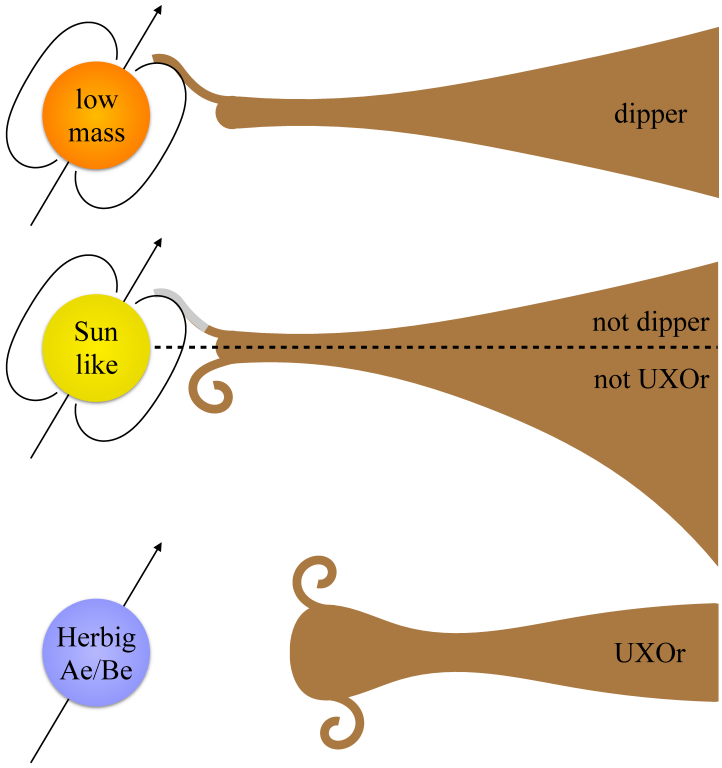

Figure 11. Cartoon showing possible origins of dippers and UXors, and why Sun-like stars may only rarely show analogous behaviour. In each case the star, magnetic dipole, and rotation axis are shown at the left (the stellar magnetic field is not necessarily always tilted with respect to the disk). Possible disk structures viewed edge-on to the right. (*top*) low-mass stars (dippers) are occulted by co-rotating material that is accreting on to the star, and the dust sublimation radius is interior to corotation [34]. (*middle*) Sun-like stars are rarely seen as dippers or UXors because i) dust sublimates outside corotation (represented by the grey accretion column in the upper half [34]), or ii) material lifted by turbulence is shadowed by the outer disk (spiral in the lower half). (*bottom*) Herbig Ae/Be stars (UXors) are occulted by turbulence that appears above self-shadowed disks [33].

In this context the rarity of RZ Psc-like objects can be explained in two ways. The first simply sidesteps the above discussion by interpreting the disk as a gas-poor asteroid belt analogue. Examples of such bright disks at a few au are rare [10], and only a subset of these will be oriented such that dimming events are seen above the disk mid plane (recalling that the occulting bodies are at tens to hundreds of stellar radii). The second explanation relies on RZ Psc's age and SED, which suggest that it hosts a gas-rich transition disk that is well settled (i.e. not significantly flared), and hence turbulence above the disk inner edge is visible. The non-detection of RZ Psc in the far-IR (Figure 10) might also be the result of such settling, and suggests that the brightness at millimeter wavelengths might be brighter than expected given the mid/far-IR brightness (e.g. [89,99]). The rarity is again explained by an unlikely geometry, and perhaps that the period during which the inner disk can be seen above the outer disk as it settles is relatively short.

6. Summary and Conclusions

Long considered a member of the UXor class of variables, RZ Psc is almost completely occulted by dust for several days, multiple times during each observing season. The "typical" UXor (which is generally a Herbig Ae object) shows day to month long dimming events that are thought to

be caused by hydrodynamic turbulence above the disk inner rim, and where the outer disk is self-shadowed [33]. Various anomalous characteristics distinguish RZ Psc from other UXors; the possible age of a few tens of Myr, the K0V spectral type, the few-day long dimming events, and the location of the IR-excess emitting dust well beyond the sublimation radius. These characteristics have been used by de Wit et al. [40] to suggest that RZ Psc hosts a gas-poor asteroid belt analogue at 0.4-0.7au and that the dust clumps that occult the star are the dispersed fragments produced in destructive planetesimal collisions.

To take a critical look at this intriguing scenario, we have presented and analysed ten years of WASP and KELT-North photometric monitoring of RZ Psc. We found circumstantial evidence that some dimming events repeat and have a semi-major axis consistent with that inferred from the IR excess, but the signal is not significant (1-2σ). The light curve gradients are consistent with this picture, but the constraints are poor. The statistics of the light curve gradients suggest that a typical dimming event has an egress rate that is initially faster, and then slower, than ingress. While this evolution seems qualitatively consistent with the structure expected from a planetesimal collision, quantitative models are needed.

By considering the joint constraints allowed by the light curve and the IR excess, we find that the objects causing the dimming events are unlikely to be representative of the structure causing the IR excess. The two can only be reconciled if the IR excess originates in a spherical shell of clumpy but on average optically thin dust, a scenario disfavoured by the increased polarisation during deep dimming events. Assuming a disk-like structure, the belt is almost certainly optically thick with an opening angle of a few tens of degrees, with the system viewed at an inclination that allows clumps residing above this belt to pass in front of the star. While such a geometry is possible for both UXor-like and asteroid belt scenarios, the relatively cool temperature of the dust around RZ Psc means that if it hosts a gas-rich disk it must be a transition object. Indeed, comparison of RZ Psc's spectrum with other objects suggest that it is similar to objects whose status is ambiguous, and could be either debris or transition disks. The low far-IR disk luminosity could arise if the outer disk is shadowed (as suggested for UXors), or simply because there is no outer disk. The spectrum is poorly sampled and would benefit from millimeter photometry, specifically to test whether there is a settled outer disk.

Overall, we conclude that the status of RZ Psc's disk is uncertain, and therefore that so is the origin of the clumps. The lack of near-IR excess shows that the disk is beyond the primordial phase, but could be in the final throes of dispersal and the occulting structures a related phenomenon. Several specific observations would help: i) mid-IR spectral monitoring would allow comparisons with transition disk systems that show "see-saw" variability, ii) continuous photometry (ideally with multiple colours) would yield the detailed shape of individual dimming events and in some cases the distribution of dust size across the clump.

As a young Sun-like star showing disk-related stellar variability, RZ Psc is a rarity. The reason may be twofold; i) the sublimation radius is greater than for low-mass stars so any accretion streams are transparent, and/or ii) in contrast to more massive stars, turbulence above the inner rim may be shadowed by the outer disk. While the asteroid belt scenario avoids the need to consider primordial disk structure, in the context of such models RZ Psc-like variability could be explained by the evolved state of the disk, which may have settled enough that the inner rim is visible.

Data and code: Materials used in the preparation of this contribution can be found online at https://github.com/drgmk/rzpsc.

Competing interests: We declare that we have no competing interests.

Contributions: GMK initiated the project, collated data, did most of the analysis, and wrote the paper. MAK contributed to the time-series analysis and conceived the iterative event finding method. KGS provided independent SED models to test for a UV excess. As members of the KELT collaboration, JP, JER, RJS, and KGS acquired the time-series photometry. MCW was a co-I on the

proposal to obtain the VISIR data. All co-authors provided input on the style and content of the manuscript.

Acknowledgments: We thank Joachim Gürtler for sharing photometry from the Sonneberg and Harvard Plates in a palatable form, AAVSO observers for monitoring RZ Psc, and Simon Hodgkin and Jim Pringle for useful discussions. This paper makes use of data from the DR1 of the WASP data [49] as provided by the WASP consortium, and the computing and storage facilities at the CERIT Scientific Cloud, reg. no. CZ.1.05/3.2.00/08.0144 which is operated by Masaryk University, Czech Republic.

Funding: GMK is supported by the Royal Society as a Royal Society University Research Fellow. JER is funded as a Future Faculty Leaders Fellow at the Harvard-Smithsonian Center for Astrophysics. MCW acknowledges support from the European Union through ERC grant number 279973. Early work on KELT-North was supported by NASA Grant NNG04GO70G.

References

1. Haisch KE Jr, Lada EA, Lada CJ.
   Disk Frequencies and Lifetimes in Young Clusters.
   ApJ. 2001 Jun;553:L153–L156.
   Available from: http://adsabs.harvard.edu/abs/2001ApJ...553L.153H.
2. Backman DE, Paresce F.
   Main-sequence stars with circumstellar solid material - The VEGA phenomenon.
   In: Levy EH, Lunine JI, editors. Protostars and Planets III; 1993. p. 1253–1304.
   Available from: http://adsabs.harvard.edu/abs/1993prpl.conf.1253B.
3. Wyatt MC, Dent WRF.
   Collisional processes in extrasolar planetesimal discs - dust clumps in Fomalhaut's debris disc.
   MNRAS. 2002 Aug;334:589–607.
   Available from: http://adsabs.harvard.edu/abs/2002MNRAS.334..589W.
4. Krivov AV.
   Debris disks: seeing dust, thinking of planetesimals and planets.
   Research in Astronomy and Astrophysics. 2010 May;10:383–414.
   Available from: http://adsabs.harvard.edu/abs/2010RAA....10..383K.
5. Fabrycky D, Tremaine S.
   Shrinking Binary and Planetary Orbits by Kozai Cycles with Tidal Friction.
   ApJ. 2007 Nov;669:1298–1315.
   Available from: http://adsabs.harvard.edu/abs/2007ApJ...669.1298F.
6. Rasio FA, Ford EB.
   Dynamical instabilities and the formation of extrasolar planetary systems.
   Science. 1996 Nov;274:954–956.
   Available from: http://adsabs.harvard.edu/abs/1996Sci...274..954R.
7. Tsiganis K, Gomes R, Morbidelli A, Levison HF.
   Origin of the orbital architecture of the giant planets of the Solar System.
   Nature. 2005 May;435:459–461.
   Available from: http://adsabs.harvard.edu/abs/2005Natur.435..459T.
8. Melis C, Zuckerman B, Rhee JH, Song I.
   The Age of the HD 15407 System and The Epoch of Final Catastrophic Mass Accretion onto Terrestrial Planets Around Sun-like Stars.
   ApJ. 2010 Jul;717:L57–L61.
   Available from: http://adsabs.harvard.edu/abs/2010ApJ...717L..57M.
9. Jackson AP, Wyatt MC.
   Debris from terrestrial planet formation: the Moon-forming collision.
   MNRAS. 2012 Sep;425:657–679.
   Available from: http://adsabs.harvard.edu/abs/2012MNRAS.425..657J.
10. Kennedy GM, Wyatt MC.
    The bright end of the exo-Zodi luminosity function: disc evolution and implications for exo-Earth detectability.
    MNRAS. 2013 Aug;433:2334–2356.

Available from: http://adsabs.harvard.edu/abs/2013MNRAS.433.2334K.
11. Booth M, Wyatt MC, Morbidelli A, Moro-Martín A, Levison HF.
The history of the Solar system's debris disc: observable properties of the Kuiper belt.
MNRAS. 2009 Oct;399:385–398.
Available from: http://adsabs.harvard.edu/abs/2009MNRAS.399..385B.
12. Kennedy GM, Murphy SJ, Lisse CM, Ménard F, Sitko ML, Wyatt MC, et al.
Evolution from protoplanetary to debris discs: the transition disc around HD 166191.
MNRAS. 2014 Mar;438:3299–3309.
Available from: http://adsabs.harvard.edu/abs/2014MNRAS.438.3299K.
13. Meng HYA, Su KYL, Rieke GH, Stevenson DJ, Plavchan P, Rujopakarn W, et al.
Large impacts around a solar-analog star in the era of terrestrial planet formation.
Science. 2014 Aug;345:1032–1035.
Available from: http://adsabs.harvard.edu/abs/2014Sci...345.1032M.
14. Joy AH.
T Tauri Variable Stars.
ApJ. 1945 Sep;102:168.
Available from: http://adsabs.harvard.edu/abs/1945ApJ...102..168J.
15. Herbst W, Herbst DK, Grossman EJ, Weinstein D.
Catalogue of UBVRI photometry of T Tauri stars and analysis of the causes of their variability.
AJ. 1994 Nov;108:1906–1923.
Available from: http://adsabs.harvard.edu/abs/1994AJ....108.1906H.
16. Morales-Calderón M, Stauffer JR, Hillenbrand LA, Gutermuth R, Song I, Rebull LM, et al.
Ysovar: The First Sensitive, Wide-area, Mid-infrared Photometric Monitoring of the Orion Nebula Cluster.
ApJ. 2011 May;733:50.
Available from: http://adsabs.harvard.edu/abs/2011ApJ...733...50M.
17. Cody AM, Stauffer J, Baglin A, Micela G, Rebull LM, Flaccomio E, et al.
CSI 2264: Simultaneous Optical and Infrared Light Curves of Young Disk-bearing Stars in NGC 2264 with CoRoT and Spitzer — Evidence for Multiple Origins of Variability.
AJ. 2014 Apr;147:82.
Available from: http://adsabs.harvard.edu/abs/2014AJ....147...82C.
18. Mamajek EE, Quillen AC, Pecaut MJ, Moolekamp F, Scott EL, Kenworthy MA, et al.
Planetary Construction Zones in Occultation: Discovery of an Extrasolar Ring System Transiting a Young Sun-like Star and Future Prospects for Detecting Eclipses by Circumsecondary and Circumplanetary Disks.
AJ. 2012 Mar;143:72.
Available from: http://adsabs.harvard.edu/abs/2012AJ....143...72M.
19. Rodriguez JE, Pepper J, Stassun KG, Siverd RJ, Cargile P, Beatty TG, et al.
Occultation of the T Tauri Star RW Aurigae A by its Tidally Disrupted Disk.
AJ. 2013 Nov;146:112.
Available from: http://adsabs.harvard.edu/abs/2013AJ....146..112R.
20. Finkenzeller U, Mundt R.
The Herbig Ae/Be stars associated with nebulosity.
A&AS. 1984 Jan;55:109–141.
Available from: http://adsabs.harvard.edu/abs/1984A&AS...55..109F.
21. Herbst W, Shevchenko VS.
A Photometric Catalog of Herbig AE/BE Stars and Discussion of the Nature and Cause of the Variations of UX Orionis Stars.
AJ. 1999 Aug;118:1043–1060.
Available from: http://adsabs.harvard.edu/abs/1999AJ....118.1043H.
22. Natta A, Whitney BA.
Models of scattered light in UXORs.
A&A. 2000 Dec;364:633–640.
Available from: http://adsabs.harvard.edu/abs/2000A&A...364..633N.
23. Bouvier J, Grankin K, Ellerbroek LE, Bouy H, Barrado D.
AA Tauri's sudden and long-lasting deepening: enhanced extinction by its circumstellar disk.
A&A. 2013 Sep;557:A77.
Available from: http://adsabs.harvard.edu/abs/2013A&A...557A..77B.

24. Rodriguez JE, Pepper J, Stassun KG, Siverd RJ, Cargile P, Weintraub DA, et al.
V409 Tau as Another AA Tau: Photometric Observations of Stellar Occultations by the Circumstellar Disk.
AJ. 2015 Jul;150:32.
Available from: http://adsabs.harvard.edu/abs/2015AJ....150...32R.
25. Mikolajewski M, Graczyk D.
Is the eclipsing variable EE CEP a cousin of epsilon Aur?
MNRAS. 1999 Mar;303:521–524.
Available from: http://adsabs.harvard.edu/abs/1999MNRAS.303..521M.
26. Dong S, Katz B, Prieto JL, Udalski A, Kozlowski S, Street RA, et al.
OGLE-LMC-ECL-11893: The Discovery of a Long-period Eclipsing Binary with a Circumstellar Disk.
ApJ. 2014 Jun;788:41.
Available from: http://adsabs.harvard.edu/abs/2014ApJ...788...41D.
27. Kloppenborg BK, Stencel RE, Monnier JD, Schaefer GH, Baron F, Tycner C, et al.
Interferometry of ϵ Aurigae: Characterization of the Asymmetric Eclipsing Disk.
ApJS. 2015 Sep;220:14.
Available from: http://adsabs.harvard.edu/abs/2015ApJS..220...14K.
28. Grinin VP.
On the Blue Emission Visible during Deep Minima of Young Irregular Variables.
Soviet Astronomy Letters. 1988 Feb;14:27.
Available from: http://adsabs.harvard.edu/abs/1988SvAL...14...27G.
29. Rostopchina AN, Grinin VP, Shakhovskoi DN.
Photometry and Polarimetry of the Classical Herbig Ae Star VV Ser.
Astronomy Reports. 2001 Jan;45:51–59.
Available from: http://adsabs.harvard.edu/abs/2001ARep...45...51R.
30. Bouvier J, Chelli A, Allain S, Carrasco L, Costero R, Cruz-Gonzalez I, et al.
Magnetospheric accretion onto the T Tauri star AA Tauri. I. Constraints from multisite spectrophotometric monitoring.
A&A. 1999 Sep;349:619–635.
Available from: http://adsabs.harvard.edu/abs/1999A&A...349..619B.
31. Grinin VP.
Polarimetric activity of Herbig Ae/Be stars.
In: The PS, Perez MR, van den Heuvel EPJ, editors. The Nature and Evolutionary Status of Herbig Ae/Be Stars. vol. 62 of Astronomical Society of the Pacific Conference Series; 1994. p. 63.
Available from: http://adsabs.harvard.edu/abs/1994ASPC...62...63G.
32. Ansdell M, Gaidos E, Rappaport SA, Jacobs TL, LaCourse DM, Jek KJ, et al.
Young "Dipper" Stars in Upper Sco and Oph Observed by K2.
ApJ. 2016 Jan;816:69.
Available from: http://adsabs.harvard.edu/abs/2016ApJ...816...69A.
33. Dullemond CP, van den Ancker ME, Acke B, van Boekel R.
Explaining UX Orionis Star Variability with Self-shadowed Disks.
ApJ. 2003 Sep;594:L47–L50.
Available from: http://adsabs.harvard.edu/abs/2003ApJ...594L..47D.
34. Bodman EHL, Quillen AC, Ansdell M, Hippke M, Boyajian TS, Mamajek EE, et al.
Dippers and Dusty Disks Edges: A Unified Model.
ArXiv e-prints. 2016 May;Available from: http://adsabs.harvard.edu/abs/2016arXiv160503985B.
35. Millan-Gabet R, Malbet F, Akeson R, Leinert C, Monnier J, Waters R.
The Circumstellar Environments of Young Stars at AU Scales.
Protostars and Planets V. 2007;p. 539–554.
Available from: http://adsabs.harvard.edu/abs/2007prpl.conf..539M.
36. Zajtseva GV.
Photometric features of RZ Piscium.
Peremennye Zvezdy. 1985;22:181–190.
Available from: http://adsabs.harvard.edu/abs/1985PZ.....22..181Z.
37. Gürtler J, Friedemann C, Reimann HG, Splittgerber E, Rudolph E.
A comparative study of the long-term light variations of six young irregular variables.

A&AS. 1999 Dec;140:293–307.
Available from: http://adsabs.harvard.edu/abs/1999A&AS..140..293G.
38. Shakhovskoi DN, Grinin VP, Rostopchina AN.
Photometric and Polarimetric Activity of RZ Psc.
Astronomy Reports. 2003 Jul;47:580–586.
Available from: http://adsabs.harvard.edu/abs/2003ARep...47..580S.
39. Grinin VP, Potravnov IS, Musaev FA.
The evolutionary status of the UX Orionis star RZ Piscium.
A&A. 2010 Dec;524:A8.
Available from: http://adsabs.harvard.edu/abs/2010A&A...524A...8G.
40. de Wit WJ, Grinin VP, Potravnov IS, Shakhovskoi DN, Müller A, Moerchen M.
Active asteroid belt causes the UXOR phenomenon in RZ Piscium.
A&A. 2013 May;553:L1.
Available from: http://adsabs.harvard.edu/abs/2013A&A...553L...1D.
41. Kardopolov VI, Sakhanenok VV, Shutemova NA.
On the character of brightness variations of RZ Pisces.
Peremennye Zvezdy. 1980;21:310–313.
Available from: http://adsabs.harvard.edu/abs/1980PZ.....21..310K.
42. Pugach AF.
Phenomenological model of the antiflare star RZ PSC.
Astrofizika. 1981 Jan;17:87–96.
Available from: http://adsabs.harvard.edu/abs/1981Afz....17...87P.
43. Pugach AF.
Optical Properties of the Circumstellar Dust around Stars with Aperiodic Fadings.
Astronomy Reports. 2004 Jun;48:470–475.
Available from: http://adsabs.harvard.edu/abs/2004ARep...48..470P.
44. Kiselev NN, Minikulov NK, Chernova GP.
Strong increase of the linear polarization of RZ PSC at deep minimum.
Astrofizika. 1991;34:333–343.
Available from: http://adsabs.harvard.edu/abs/1991Afz....34..333K.
45. Potravnov IS, Grinin VP, Ilyin IV, Shakhovskoy DN.
An in-depth analysis of the RZ Piscium atmosphere.
A&A. 2014 Mar;563:A139.
Available from: http://adsabs.harvard.edu/abs/2014A&A...563A.139P.
46. Kóspál Á, Moór A, Juhász A, Ábrahám P, Apai D, Csengeri T, et al.
ALMA Observations of the Molecular Gas in the Debris Disk of the 30 Myr Old Star HD 21997.
ApJ. 2013 Oct;776:77.
Available from: http://adsabs.harvard.edu/abs/2013ApJ...776...77K.
47. Rostopchina AN, Grinin VP, Shakhovskoi DN.
Cyclic variability of UX Ori Stars: UX Ori, SV Cep, and RZ Psc.
Astronomy Letters. 1999 Apr;25:243–249.
Available from: http://adsabs.harvard.edu/abs/1999AstL...25..243R.
48. Pollacco DL, Skillen I, Collier Cameron A, Christian DJ, Hellier C, Irwin J, et al.
The WASP Project and the SuperWASP Cameras.
PASP. 2006 Oct;118:1407–1418.
Available from: http://adsabs.harvard.edu/abs/2006PASP..118.1407P.
49. Butters OW, West RG, Anderson DR, Collier Cameron A, Clarkson WI, Enoch B, et al.
The first WASP public data release.
A&A. 2010 Sep;520:L10.
Available from: http://adsabs.harvard.edu/abs/2010A&A...520L..10B.
50. Pepper J, Pogge RW, DePoy DL, Marshall JL, Stanek KZ, Stutz AM, et al.
The Kilodegree Extremely Little Telescope (KELT): A Small Robotic Telescope for Large-Area Synoptic Surveys.
PASP. 2007 Aug;119:923–935.
Available from: http://adsabs.harvard.edu/abs/2007PASP..119..923P.
51. Karetnikov VG, Pugach AF.
A Flare of Anti-Flare Star RZ Psc.
Information Bulletin on Variable Stars. 1973 Apr;783:1.

Available from: http://adsabs.harvard.edu/abs/1973IBVS..783....1K.
52. Pojmanski G.
The All Sky Automated Survey.
Acta Astron.. 1997 Oct;47:467–481.
Available from: http://adsabs.harvard.edu/abs/1997AcA....47..467P.
53. Potravnov IS, Gorynya NA, Grinin VP, Minikulov NK.
Radial Velocity Fluctuations of RZ Psc.
Astrophysics. 2014 Dec;57:491–499.
Available from: http://adsabs.harvard.edu/abs/2014Ap.....57..491P.
54. van Werkhoven TIM, Kenworthy MA, Mamajek EE.
Analysis of 1SWASP J140747.93-394542.6 eclipse fine-structure: hints of exomoons.
MNRAS. 2014 Jul;441:2845–2854.
Available from: http://adsabs.harvard.edu/abs/2014MNRAS.441.2845V.
55. Siverd RJ, Beatty TG, Pepper J, Eastman JD, Collins K, Bieryla A, et al.
KELT-1b: A Strongly Irradiated, Highly Inflated, Short Period, 27 Jupiter-mass Companion Transiting a Mid-F Star.
ApJ. 2012 Dec;761:123.
Available from: http://adsabs.harvard.edu/abs/2012ApJ...761..123S.
56. Geers VC, van Dishoeck EF, Visser R, Pontoppidan KM, Augereau JC, Habart E, et al.
Spatially extended polycyclic aromatic hydrocarbons in circumstellar disks around T Tauri and Herbig Ae stars.
A&A. 2007 Dec;476:279–289.
Available from: http://adsabs.harvard.edu/abs/2007A&A...476..279G.
57. Verhoeff AP, Waters LBFM, van den Ancker ME, Min M, Stap FA, Pantin E, et al.
A mid-IR study of the circumstellar environment of Herbig Be stars.
A&A. 2012 Feb;538:A101.
Available from: http://adsabs.harvard.edu/abs/2012A&A...538A.101V.
58. Espaillat C, Furlan E, D'Alessio P, Sargent B, Nagel E, Calvet N, et al.
A Spitzer IRS Study of Infrared Variability in Transitional and Pre-transitional Disks Around T Tauri Stars.
ApJ. 2011 Feb;728:49.
Available from: http://adsabs.harvard.edu/abs/2011ApJ...728...49E.
59. Flaherty KM, Muzerolle J, Rieke G, Gutermuth R, Balog Z, Herbst W, et al.
Infrared Variability of Evolved Protoplanetary Disks: Evidence for Scale Height Variations in the Inner Disk.
ApJ. 2012 Mar;748:71.
Available from: http://adsabs.harvard.edu/abs/2012ApJ...748...71F.
60. Beichman CA, Bryden G, Gautier TN, Stapelfeldt KR, Werner MW, Misselt K, et al.
An Excess Due to Small Grains around the Nearby K0 V Star HD 69830: Asteroid or Cometary Debris?
ApJ. 2005 Jun;626:1061–1069.
Available from: http://adsabs.harvard.edu/abs/2005ApJ...626.1061B.
61. Song I, Zuckerman B, Weinberger AJ, Becklin EE.
Extreme collisions between planetesimals as the origin of warm dust around a Sun-like star.
Nature. 2005 Jul;436:363–365.
Available from: http://adsabs.harvard.edu/abs/2005Natur.436..363S.
62. Olofsson J, Juhász A, Henning T, Mutschke H, Tamanai A, Moór A, et al.
Transient dust in warm debris disks. Detection of Fe-rich olivine grains.
A&A. 2012 Jun;542:A90.
Available from: http://adsabs.harvard.edu/abs/2012A&A...542A..90O.
63. Wright EL, et al.
The Wide-field Infrared Survey Explorer (WISE): Mission Description and Initial On-orbit Performance.
AJ. 2010 Dec;140:1868–1881.
Available from: http://adsabs.harvard.edu/abs/2010AJ....140.1868W.
64. Mainzer A, Bauer J, Cutri RM, Grav T, Masiero J, Beck R, et al.
Initial Performance of the NEOWISE Reactivation Mission.
ApJ. 2014 Sep;792:30.

Available from: http://adsabs.harvard.edu/abs/2014ApJ...792...30M.
65. Zhang K, Isella A, Carpenter JM, Blake GA.
Comparison of the Dust and Gas Radial Structure in the Transition Disk [PZ99] J160421.7-213028.
ApJ. 2014 Aug;791:42.
Available from: http://adsabs.harvard.edu/abs/2014ApJ...791...42Z.
66. Meng HYA, Rieke GH, Su KYL, Ivanov VD, Vanzi L, Rujopakarn W.
Variability of the Infrared Excess of Extreme Debris Disks.
ApJ. 2012 May;751:L17.
Available from: http://adsabs.harvard.edu/abs/2012ApJ...751L..17M.
67. Melis C, Zuckerman B, Rhee JH, Song I, Murphy SJ, Bessell MS.
Rapid disappearance of a warm, dusty circumstellar disk.
Nature. 2012 Jul;487:74–76.
Available from: http://adsabs.harvard.edu/abs/2012Natur.487...74M.
68. Edelson RA, Krolik JH.
The discrete correlation function - A new method for analyzing unevenly sampled variability data.
ApJ. 1988 Oct;333:646–659.
Available from: http://adsabs.harvard.edu/abs/1988ApJ...333..646E.
69. Winn JN, Hamilton CM, Herbst WJ, Hoffman JL, Holman MJ, Johnson JA, et al.
The Orbit and Occultations of KH 15D.
ApJ. 2006 Jun;644:510–524.
Available from: http://adsabs.harvard.edu/abs/2006ApJ...644..510W.
70. Kenworthy MA, Mamajek EE.
Modeling Giant Extrasolar Ring Systems in Eclipse and the Case of J1407b: Sculpting by Exomoons?
ApJ. 2015 Feb;800:126.
Available from: http://adsabs.harvard.edu/abs/2015ApJ...800..126K.
71. Potravnov IS, Grinin VP.
On the kinematic age of RZ Psc.
Astronomy Letters. 2013 Nov;39:776–780.
Available from: http://adsabs.harvard.edu/abs/2013AstL...39..776P.
72. Siess L, Dufour E, Forestini M.
An internet server for pre-main sequence tracks of low- and intermediate-mass stars.
A&A. 2000 Jun;358:593–599.
Available from: http://adsabs.harvard.edu/abs/2000A&A...358..593S.
73. Potravnov IS, Grinin VP, Ilyin IV.
Observation of Circumstellar Gas in the Neighborhood of RZ Psc.
Astrophysics. 2013 Dec;56:453–460.
Available from: http://adsabs.harvard.edu/abs/2013Ap.....56..453P.
74. Kaminskiĭ BM, Kovalchuk GU, Pugach AF.
Spectral Features of RZ Psc, a Cool Star with Algol-like Brightness Minima.
Astronomy Reports. 2000 Sep;44:611–623.
Available from: http://adsabs.harvard.edu/abs/2000ARep...44..611K.
75. Scholz A, Mužić K, Geers V.
The young low-mass star ISO-Oph-50: extreme variability induced by a clumpy, evolving circumstellar disc.
MNRAS. 2015 Jul;451:26–33.
Available from: http://adsabs.harvard.edu/abs/2015MNRAS.451...26S.
76. Natta A, Grinin VP, Mannings V, Ungerechts H.
The Evolutionary Status of UX Orionis-Type Stars.
ApJ. 1997 Dec;491:885–890.
Available from: http://adsabs.harvard.edu/abs/1997ApJ...491..885N.
77. Caballero JA.
The occultation events of the Herbig Ae/Be star V1247 Orionis.
A&A. 2010 Feb;511:L9.
Available from: http://adsabs.harvard.edu/abs/2010A&A...511L...9C.
78. Boyajian TS, LaCourse DM, Rappaport SA, Fabrycky D, Fischer DA, Gandolfi D, et al.

Planet Hunters IX. KIC 8462852 - where's the flux?
MNRAS. 2016 Apr;457:3988–4004.
Available from: http://adsabs.harvard.edu/abs/2016MNRAS.457.3988B.
79. Bibo EA, The PS.
The type of variability of Herbig Ae/Be stars.
A&AS. 1991 Aug;89:319–334.
Available from: http://adsabs.harvard.edu/abs/1991A&AS...89..319B.
80. Ferlet R, Vidal-Madjar A, Hobbs LM.
The Beta Pictoris circumstellar disk. V - Time variations of the CA II-K line.
A&A. 1987 Oct;185:267–270.
Available from: http://adsabs.harvard.edu/abs/1987A&A...185..267F.
81. Welsh BY, Montgomery S.
Circumstellar Gas-Disk Variability Around A-Type Stars: The Detection of Exocomets?
PASP. 2013 Jul;125:759–774.
Available from: http://adsabs.harvard.edu/abs/2013PASP..125..759W.
82. Kiefer F, Lecavelier des Etangs A, Augereau JC, Vidal-Madjar A, Lagrange AM, Beust H.
Exocomets in the circumstellar gas disk of HD 172555.
A&A. 2014 Jan;561:L10.
Available from: http://adsabs.harvard.edu/abs/2014A&A...561L..10K.
83. Beust H, Vidal-Madjar A, Ferlet R, Lagrange-Henri AM.
The Beta Pictoris circumstellar disk. X - Numerical simulations of infalling evaporating bodies.
A&A. 1990 Sep;236:202–216.
Available from: http://adsabs.harvard.edu/abs/1990A&A...236..202B.
84. Beust H, Morbidelli A.
Mean-Motion Resonances as a Source for Infalling Comets toward β Pictoris.
Icarus. 1996 Apr;120:358–370.
Available from: http://adsabs.harvard.edu/abs/1996Icar..120..358B.
85. Calvet N, D'Alessio P, Watson DM, Franco-Hernández R, Furlan E, Green J, et al.
Disks in Transition in the Taurus Population: Spitzer IRS Spectra of GM Aurigae and DM Tauri.
ApJ. 2005 Sep;630:L185–L188.
Available from: http://adsabs.harvard.edu/abs/2005ApJ...630L.185C.
86. Schneider A, Song I, Melis C, Zuckerman B, Bessell M, Hufford T, et al.
The Nearby, Young, Isolated, Dusty Star HD 166191.
ApJ. 2013 Nov;777:78.
Available from: http://adsabs.harvard.edu/abs/2013ApJ...777...78S.
87. Chen CH, Sargent BA, Bohac C, Kim KH, Leibensperger E, Jura M, et al.
Spitzer IRS Spectroscopy of IRAS-discovered Debris Disks.
ApJS. 2006 Sep;166:351–377.
Available from: http://adsabs.harvard.edu/abs/2006ApJS..166..351C.
88. Rodgers-Lee D, Scholz A, Natta A, Ray T.
The Herschel view of circumstellar discs: a multiwavelength study of Chamaeleon-I.
MNRAS. 2014 Sep;443:1587–1600.
Available from: http://adsabs.harvard.edu/abs/2014MNRAS.443.1587R.
89. Dullemond CP, Dominik C.
The effect of dust settling on the appearance of protoplanetary disks.
A&A. 2004 Jul;421:1075–1086.
Available from: http://adsabs.harvard.edu/abs/2004A&A...421.1075D.
90. Olofsson J, Henning T, Nielbock M, Augereau JC, Juhàsz A, Oliveira I, et al.
The twofold debris disk around HD 113766 A. Warm and cold dust as seen with VLTI/MIDI and Herschel/PACS.
A&A. 2013 Mar;551:A134.
Available from: http://adsabs.harvard.edu/abs/2013A&A...551A.134O.
91. Martin C, Barlow T, Barnhart W, Bianchi L, Blakkolb BK, Bruno D, et al.
The Galaxy Evolution Explorer.
In: Blades JC, Siegmund OHW, editors. Future EUV/UV and Visible Space Astrophysics Missions and Instrumentation.. vol. 4854 of Proc. SPIE; 2003. p. 336–350.

Available from: http://adsabs.harvard.edu/abs/2003SPIE.4854..336M.
92. Calvet N, Gullbring E.
The Structure and Emission of the Accretion Shock in T Tauri Stars.
ApJ. 1998 Dec;509:802–818.
Available from: http://adsabs.harvard.edu/abs/1998ApJ...509..802C.
93. Cutri RM, et al.
2MASS All Sky Catalog of point sources.; 2003.
Available from: http://adsabs.harvard.edu/abs/2003tmc..book.....C.
94. Brott I, Hauschildt PH.
A PHOENIX Model Atmosphere Grid for Gaia.
In: Turon C, O'Flaherty KS, Perryman MAC, editors. The Three-Dimensional Universe with Gaia. vol. 576 of ESA Special Publication; 2005. p. 565.
Available from: http://adsabs.harvard.edu/abs/2005ESASP.576..565B.
95. Meng HYA, Su KYL, Rieke GH, Rujopakarn W, Myers G, Cook M, et al.
Planetary Collisions Outside the Solar System: Time Domain Characterization of Extreme Debris Disks.
ApJ. 2015 May;805:77.
Available from: http://adsabs.harvard.edu/abs/2015ApJ...805...77M.
96. Szűcs L, Apai D, Pascucci I, Dullemond CP.
Stellar-mass-dependent Disk Structure in Coeval Planet-forming Disks.
ApJ. 2010 Sep;720:1668–1673.
Available from: http://adsabs.harvard.edu/abs/2010ApJ...720.1668S.
97. Ansdell M, Gaidos E, Williams JP, Kennedy G, Wyatt MC, LaCourse DM, et al.
Dipper discs not inclined towards edge-on orbits.
MNRAS. 2016 Oct;462:L101–L105.
Available from: http://adsabs.harvard.edu/abs/2016MNRAS.462L.101A.
98. Kenyon SJ, Hartmann L.
Spectral energy distributions of T Tauri stars - Disk flaring and limits on accretion.
ApJ. 1987 Dec;323:714–733.
Available from: http://adsabs.harvard.edu/abs/1987ApJ...323..714K.
99. Dullemond CP, Hollenbach D, Kamp I, D'Alessio P.
Models of the Structure and Evolution of Protoplanetary Disks.
Protostars and Planets V. 2007;p. 555–572.
Available from: http://adsabs.harvard.edu/abs/2007prpl.conf..555D.